DEPOSITION ANALYSIS OF UNATTACHED RADON DECAY PRODUCTS IN HUMAN RESPIRATORY TRACT

By

Abdu Seid Kamil

A THESIS SUBMITTED TO

THE PROGRAM OF GRADUATE STUDIES OF
ADDIS ABABA UNIVERSITY

IN PARTIAL FULFILLMENT OF THE REQUIREMENTS
FOR THE DEGREE

MASTER OF SCIENCE in PHYSICS

ADDIS ABABA, ETHIOPIA

JULY 2018

ADDIS ABABA UNIVERSITY

PROGRAM OF GRADUATE STUDIES

DEPOSITION ANALYSIS OF UNATTACHED RADON DECAY PRODUCTS IN HUMAN RESPIRATORY TRACT

By

Abdu Seid Kamil

Department of Physics

Addis Ababa University

Approved by the Examining Board:

Dr. Tilahun Tesfaye Signature _____
Advisor

Professor A.K. Chaubey Signature _____
Examiner

Dr. Belayneh Mesfin Signature _____
Examiner

Dated: July 2018

ADDIS ABABA UNIVERSITY

Date: **July 2018**

Author: **Abdu Seid Kamil**

Title: **Deposition analysis of unattached radon decay products in human respiratory tract**

Department: **Department of Physics**

Degree: **M.Sc.** Convocation: **July** Year: **2018**

Permission is herewith granted to Addis Ababa University to circulate and to have copied for non-commercial purposes, at its discretion, the above title upon the request of individuals or institutions.

_____

Signature of Author

This Work is Dedicated

to

My Mother

Table of Contents

List of Tables

List of Figures

Acknowledgements

I would like to express my special appreciation and thanks to my advisor, Dr. Tilahun Tesfaye, for the guidance, encouragement, and advice he has provided to complete the present research work successfully. Your advice on both research as well as on my career have been invaluable.

In particular I would like to thank Professor Dragoslav Nikezic from Montenegro, Serbia (Eastern Europe), for his kindness to provide the Fortran program which is used to calculate the dose conversion factor (DCF) for radon and its decay products.

Finally, I would like to thank all the staff members of department physics of Addis Ababa University for their support throughout the year, Addis ababa University for financial support to my thesis, and Samara University for its sponsorship to join graduate study in the field of Nuclear Physics at Addis Ababa University.

Addis Ababa University

Abdu Seid Kamil

July, 2018

Abbreviations

ICRP	International Commission on Radiological Protection
DCF	Dose Conversion Factor
mSv	millisieverts
WLM	Working Level Month
ICRP66	ICRP publication 66
HRTM	Human Respiratory Tract Model
RADEP	Radon Dose Evaluation Program
IMBA	Integrated Modules for Bioassay Analysis
RADOS	Radon Lung Dosimetry
IDEAL	Inhalation, Deposition, Exhalation of Aerosol in/from the Lungs
DNA	Deoxyribonucleic acid

Abstract

Radon is a natural radioactive gas derived from geological materials. The greatest fraction of the natural radiation exposure in human results from inhalation of the short-lived decay products of radon (^{222}Rn), which occur in the free atmosphere and in higher concentrations in the room air of buildings. Inhalation of unattached radon progeny has been implicated in potential health risks of ambient and indoor environments. These particles deposit in the respiratory tract mainly by diffusion. In this paper, the deposition pattern of unattached radon decay products in the human respiratory tract of adults Caucasian male based on ICRP66 algebraic formulas is reviewed. The percentage of deposition fractions for unattached radon progeny in respiratory tract were estimated for best estimation of aerosol parameters, with range of 49.03%–16.70% , 48.29%–19.00%, 2.25%–7.17%, 0.38%–32.04% and 0.04%–23.40% for nose, mouth, bronchial, bronchiolar and alveolar region, respectively.

CHAPTER 1
Introduction

We live in a world in which radiation is part and parcel of the natural environment [1]. That is all living organisms are exposed to ionizing radiation coming from cosmic (extra terrestrial) sources and terrestrial radionuclides that are part of the earth's crust.

Radiations of cosmic origin include ionized nuclei about 90% protons, 9% alpha particles and the rest heavier nucleon and they are distinguished by their high energies. Most cosmic rays are relativistic, having energies comparable to or somewhat greater than their masses. A very few of them have ultrarelativistic energies extending up to 1020 eV (about 20 joules), eleven orders of magnitude greater than the equivalent rest mass energy of a proton [2].

Terrestrial sources of ionizing radiation include radioactive radionuclides such as ^{238}U, ^{235}U and ^{232}Th that decay in series for billions of years since the creation of our earth itself. In addition to these series decaying radionuclides, stand alone radionuclides, such as ^{14}C, ^{40}K are also part of the radiation environment.

Exposure to radiations of cosmic origin becomes important, from radiation protection perspective, only at high altitudes and in deep space.

Exposure from radiations of terrestrial origin are mainly due to radioactive nuclides present in earth's crust, in atmosphere and in building materials. These exposure can be *external* and *internal*.

1. External exposure, as the name indicates, is exposure from outside the body and;
2. Internal exposure is caused when radionuclides are inhaled, ingested or introduced into the body along different exposure pathways.

According to the US National Council on Radiation Protection and Measurements (NCRP), the average annual radiation dose per person in the U.S. is 2.28 millisieverts. The

pie chart below shows the various radiation sources that contribute to the average annual radiation dose per person in the US [3] .

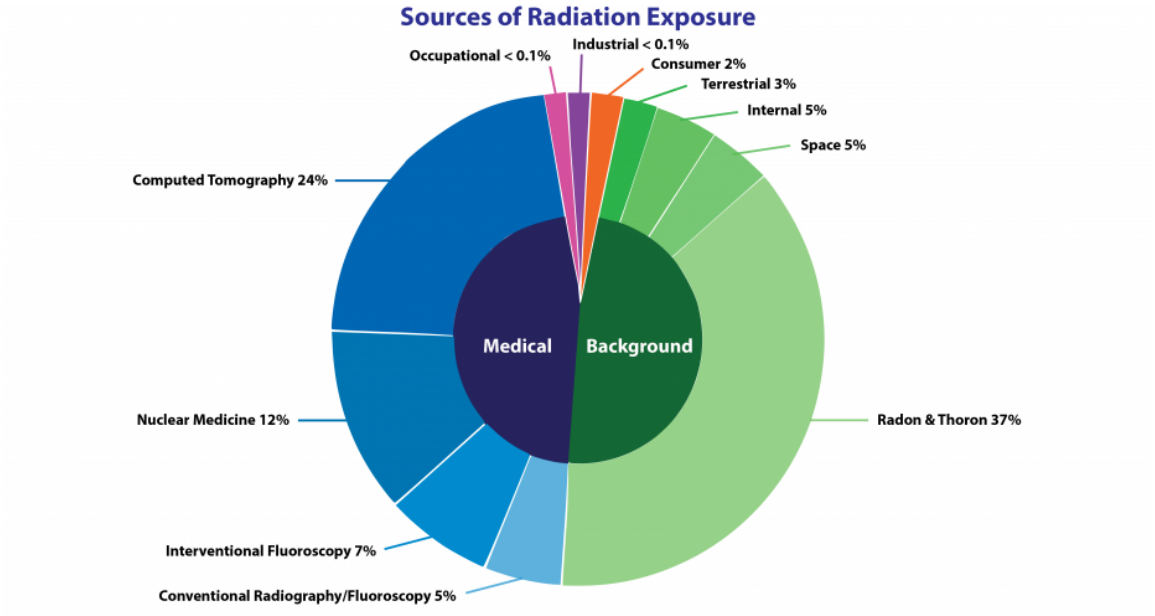

Average Annual Radiation Dose

Sources	Radon & Thoron	Computed Tomography	Nuclear Medicine	Interventional Fluoroscopy	Space	Conventional Radiography/ Fluoroscopy	Internal	Terrestrial	Consumer	Occupational	Industrial
Units											
mrem (United States)	228 mrem	147 mrem	77 mrem	43 mrem	33 mrem	33 mrem	29 mrem	21 mrem	13 mrem	0.5 mrem	0.3 mrem
mSv (International)	2.28 mSv	1.47 mSv	0.77 mSv	0.43 mSv	0.33 mSv	0.33mSv	0.29 mSv	0.21 mSv	0.13 mSv	0.005 mSv	0.003 mSv

(Source: National Council on Radiation Protection & Measurements, Report No. 160)

Figure 1.1: Percentage contribution of various sources to the average annual radiation dose per person in the US.

As can be seen from figure 1.1, the greatest fraction of the natural radiation exposure and dose to human results from inhalation of the short lived decay products of radon. The radioactive gases radon and thoron, which are created when other naturally occurring elements undergo radioactive decay, contribute nearly 40% of the dose to humans.

In Sweden it is estimated that 300-1500 lung cancer cases are induced annually by residential radon [4].

^{222}Rn gas is formed naturally in Uranium decay series. Radon is a noble gas, not bound chemically in the material where its parents resided. The half-life of ^{222}Rn (3.82 day) is long enough for much of the gas to work its way out into the atmosphere. All of the decay products of radon gas are called the radon progeny (radon daughters).

Radon is also generated in the thorium and actinium series natural series decaying elements too. The thorium series generates ^{220}Rn, which is also called thoron. ^{220}Rn has a half-life of 56 sec and therefore it has greater chance to decay before becoming

airborne. The actinium series produces ^{219}Rn, also called actinon and its half-life is only 4 sec, and its contribution to airborne radon is insignificant [5].

The health effects of ^{222}Rn decay progeny are mainly due to the deposition of the airborne decay products in the respiratory tract such that their subsequent decay leads to a dose of energy to the bronchial epithelium. In order to separate the aerodynamic behaviour of the decay products into different classes of depositional behaviour, Chamberlain and Dyson first described the highly diffusive portion for the airborne activity size distribution as the *unattached fraction* [6].

One of the important questions in trying to assess the dose resulting from a given exposure to airborne ^{222}Rn decay products is their fractional penetration through the nasal cavity and deposition in the respiratory tract.

In this work the percentage deposition of unattached fraction of radon daughters is computed by using ICRP66 algebraic formulas.

Objectives of the Study

General objective

The straightforward objective of this research is to estimate the regional deposition of unattached radon decay products in human respiratory tract for adult Caucasian male.

Specific objectives

- To determine the deposition of unattached radon daughters in each regions of human respiratory tract.
- To compare effects of the ICRP 1994 and modified parameters on deposition fraction for unattached radon decay products.

CHAPTER 2

Theoretical Background of the Study

2.1 Radon Gas Discovery and Properties

2.1.1 Discovery of radon

Radon is the heaviest of all noble gases, a class of chemically inert gases with low reactivity, and has a total of 36 isotopes ranging from ^{193}Rn to ^{228}Rn [7]. All of the isotopes are radioactive, with three isotopes that are constantly produced from the ^{238}U (^{222}Rn), ^{235}U (^{219}Rn, also known as actinon, derived from its grandparent, ^{227}Ac) and ^{232}Th (^{220}Rn, also known as thoron, derived eventually from ^{232}Th). Only four of 36 radon isotopes have half-lives greater than 1 hour. Radon was the last noble gas to be discovered by Friedrich Ernest Dorn, a German scientist in 1900 [8].

It was originally named as nitron, from the Latin word "nitens", which means shining. In 1923, it was renamed as radon. Other isotopes of radon ^{220}Rn and ^{219}Rn were discovered by R. B. Owens and E. Rutherford in 1899, and F. 0. Giesel and A. Debierne in 1904, respectively.

2.1.2 Physical Properties of Radon

Radon is a colorless gas and it is the heaviest and densest gas known in nature. Radon dissolves in water and becomes a clear, colorless liquid below its boiling point. When cooled below its freezing point, radon has a brilliant phosphorescence which becomes yellow at lower temperatures and orange-red at the temperature of liquid air [8].

The atoms of radon and other noble gases have a closed-shell electronic structure and are extremely stable, as the ionization enthalpies are high. There are no ordinary electron-pair interactions among the noble gas atoms. On the periodic table radon lies on the diagonal in between the metals and non-metals and exhibits

some of the characteristics of both groups, hence, it was suggested that radon can be classified as a metalloid element, along with boron, silicon, germanium, arsenic, antimony, tellurium, polonium and astatine [7].

In the early 1960's, a number of chemists found ways of making compounds of the noble gases. They did so by combining a noble gas with a very active element. The element generally used was fluorine, the most active chemical element. The result was the formation of noble gas compounds and the first radon compound to be produced was radon fluoride (RnF). Radon has been shown to react spontaneously at 25 ^{0}C or lower temperatures with fluorine, halogen fluorides (except IF_5). When radon is heated to 400 ^{0}C with elemental fluorine, non-volatile radon difluoride is formed:

$$Rn + F_2 \longrightarrow RnF_2 \tag{2.1}$$

Some physical and chemical properties of radon are given in Table 2.1.

Table 2.1: Physical and chemical properties of radon.

Property	Values
Atomic number	86
Standard atomic weight	222
Outer shell electron configuration	$6s^2 6p^6$
Density	9.73 kg/m^3 (at 0 ^{0}C)
Melting point (^{0}K)	202
Normal boiling point (^{0}K)	208.2
Heat of fusion (kJ/mol)	3.247
Heat of vaporization (kJ/mol)	18
First ionization enthalpy (kJ/mol)	1037
Oxidation states	0, 2, 6
Electronegativity	2.2 (Pauling scale)
Covalent radius (nm)	0.15
van der Waals radius (nm)	0.22

2.2 Theory of Radioactive Decay: Brief Review

Radioactivity is a spontaneous process of transforming unstable nuclide into a series (chain) of radioactive daughters, forming series of radionuclides that end when a stable species is produced. The disintegration take place by emission of particles, such as alpha (α), beta (β) and gamma (γ) radiation.

The basic law of radioactive decay which relates the rate at which atoms disintegrate to the number of atoms present at a given time. The result is

$$\frac{dN}{dt} = -\lambda N, \tag{2.2}$$

where N is the number of atoms present at time, t; dN is the number of atoms disintegrating in a time interval dt, and λ is the disintegration constant for a given radioactive element. The minus sign is used to indicate a decrease in N with time. Integration of equation (2.2) yields

$$N = N_0 e^{-\lambda t}, \tag{2.3}$$

where N_0 is the number of atoms present at an arbitrary initial time, $t = 0$ and N is the number present at time, t.

The activity (A) is determined by counting the alpha, beta and gamma rays from a given sample by use of appropriate detectors and electronic counting equipment. Hence, it is convenient to use equation (2.3) in the following forms:

$$A = \frac{dN}{dt} = A_0 e^{-\lambda t}, \tag{2.4}$$

where A_0 the activity at a time $t = 0$.

The number of atoms N in a pure sample of known mass of a given radioactive element can be determined if necessary from Avogadro's number and the mass number.

Alpha decay

Many heavy nuclei, especially those of the naturally occurring radioactive series, decay through alpha emission [9]. In alpha decay, a radionuclide emits a heavy, charged particle called an alpha (α) particle. An alpha particle is four times heavier than a proton or neutron and carries an electric charge that is twice that of a proton. In fact, an α particle happens to be the nucleus of a doubly ionized helium atom ($^4_2He^{2+}$). From the conservation laws of the mass number and electric charge, it follows that during alpha decay the mass number and the atomic number of the resulting nuclide (the daughter nuclide) will be reduced by 4 and 2, respectively. Alpha decay can be expressed as:

$$^A_Z X \longrightarrow ^{A-4}_{Z-2} X' + ^4_2 He + Q_\alpha, \tag{2.5}$$

where Q_α is net energy released in the decay appears as kinetic energy shared between the α-particle and the daughter nucleus and is given by:

$$Q_\alpha = (m_X - m_{X'} - m_\alpha)c^2, \tag{2.6}$$

where m refer to mass.

$$Q_\alpha = T_{X'} + T_\alpha = T_\alpha \left(\frac{A}{A-4} \right), \tag{2.7}$$

where T denotes kinetic energy, A is the mass number of the parent nucleus, and the decay will occur spontaneously only if Q > 0.

Beta decay

During this transformation, a neutron or a proton inside the nucleus of a radionuclide is converted to a proton or a neutron, respectively. Beta decay occurs through one of the following processes:

1. Beta minus decay (β^-)

   A neutron-rich parent nucleus transforms a neutron into a proton and ejects an electron e^- and anti-neutrino $\bar{\nu}$. When a neutron is converted into a proton, the positive charge inside the nucleus is increased by one, and therefore the repulsive forces between protons are increased [10].

   $$n \longrightarrow p + e^- + \bar{\nu}. \tag{2.8}$$

2. Beta plus decay (β^+)

   A proton-rich parent nucleus transforms a proton into a neutron and ejects a positron e^+ and an electronic neutrino ν. When a proton is converted into a neutron, the positive charge inside the nucleus is decreased by one, this reduce the repulsive forces between protons.

   $$p \longrightarrow n + e^+ + \nu. \tag{2.9}$$

3. Electron capture

   Occur when an atomic electron ventures inside the nuclear volume, is captured by a proton, triggers a proton to neutron transformation, and an ejection of an electronic neutrino ν.

   $$p + e^- \longrightarrow n + \nu. \tag{2.10}$$

Gamma decay

Most α and β decays, and in fact most nuclear reactions as well, leave the final nucleus in an excited state [9]. These excited states decay rapidly to the ground state through one of the following two processes:

a) By emitting the excitation energy in the form of one or more γ photons in a decay process referred to as γ decay.

$$ {}^{A}_{Z}X^{*} \longrightarrow {}^{A}_{Z}X + \gamma. \tag{2.11} $$

b) By transferring the excitation energy to one of its associated atomic orbital electrons (usually a K shell electron) in a process called internal conversion.

$$ {}^{A}_{Z}X^{*} \longrightarrow {}^{A}_{Z}X^{+} + e^{-} \longrightarrow {}^{A}_{Z}X, \tag{2.12} $$

where ${}^{A}_{Z}X^{*}$ stands for an excited state of the nucleus ${}^{A}_{Z}X$; and ${}^{A}_{Z}X^{+}$ is the singly ionized state of atom ${}^{A}_{Z}X$ following internal conversion decay.

Mean life and half-life

The expectation value of the time needed for an initial population of N_0 radioactive nuclei to decay to $1/e$ of their original number is called the mean 1ife (τ). From equation (2.2)

$$ \lambda = -\frac{dN/N}{dt}, \tag{2.13} $$

which shows that the decay constant is the fraction of atoms decaying per unit time, or the probability of decay per unit time since this is a statistical process. The reciprocal $\left(\frac{1}{\lambda}\right)$ is then the average life of the atom. In equation (2.4), τ is the value of t required for the number of atoms N in a sample to reduce by a factor of $1/e$ hence

$$ \frac{N}{N_0} = \frac{1}{e} = e^{-\lambda\tau} \tag{2.14} $$

The half-life ($t_{1/2}$) of a radioactive substance is defined as the time required for an original number of atoms N_0 to reduce to one-half that number, i.e. $N = N_0/2$. Substituting in equation (2.3) yields

$$ t_{1/2} = \frac{0.693}{\lambda} \tag{2.15} $$

2.2.1 Radioactive decay series

Most radioactive nuclides found in nature are members of naturally occurring decay series [11]. The sequence of radioactive daughter nuclides that are formed by the radioactive decay of a parent nuclide to a final, stable daughter nuclide.

When one or more of the decay products of a radioelement are themselves radioactive, a radioactive series results which with certain simplifying assumptions [12], the

general decay chain can be visualized as

$$N_1 \longrightarrow N_2 \longrightarrow N_3 \longrightarrow \cdots \longrightarrow N_{i-1} \longrightarrow N_i \quad (stable)$$

The decay and buildup equations for each member of the decay chain are

$$\frac{dN_1(t)}{dt} = -\lambda_1 N_1(t) \tag{2.16}$$
$$\frac{dN_2(t)}{dt} = \lambda_1 N_1(t) - \lambda_2 N_2(t) \tag{2.17}$$
$$\frac{dN_3(t)}{dt} = \lambda_2 N_2(t) - \lambda_3 N_3(t) \tag{2.18}$$
$$\frac{dN_{i-1}(t)}{dt} = \lambda_{i-2} N_{i-2}(t) - \lambda_{i-1} N_{i-1}(t) \tag{2.19}$$
$$\frac{dN_i(t)}{dt} = \lambda_{i-1} N_{i-1}(t) \tag{2.20}$$

where $i = 2, 3, 4 \cdots$.

The general equation giving the number of atoms of the i^{th} isotope, at time t in terms of the decay constants of all the other isotopes in the chain was developed by Bateman [13].

For the k^{th} isotope,

$$\frac{dN_k}{dt} = b_{k-1}\lambda_{k-1}N_{k-1} - \lambda_k N_k, \qquad (k = 2, 3, 4 \cdots)$$

where b_k the branching ratio.

The Bateman equation takes the form:

$$N_k(t) = N_1(0) \left(\prod_{i=1}^{k-1} b_i \lambda_i \right) \sum_{j=1}^{k} \frac{e^{-\lambda_j t}}{\prod\limits_{\substack{i=1 \\ i \neq j}}^{k} (\lambda_i - \lambda_j)} \tag{2.21}$$

For

$$N_k(0) = 0, \qquad i > 1$$

where $N_k(0)$ is the number of atoms of the k^{th} isotope of the series at time $t = 0$.

If $N_k(0)$ progeny atoms are present when $t = 0$, then equation (2.21) may be rewritten as

$$N_k(t) = N_1(0) \left(\prod_{i=1}^{k-1} b_i \lambda_i \right) \sum_{j=1}^{k} \frac{e^{-\lambda_j t}}{\prod\limits_{\substack{i=1 \\ i \neq j}}^{k} (\lambda_i - \lambda_j)} + N_k(0) e^{-\lambda_k t} \tag{2.22}$$

where N_k is the number of nuclei of the k^{th} daughter isotope, λ_k the corresponding decay constant, $N_1(0)$ the starting number of the parent nuclei and t the time since start of the decay.

Radon as Part of the Natural ^{238}U Series

In nature the 4.5 billion years half-life Uranium (^{238}U) decays into daughter radionuclides, forming a chain of radionuclides that ends with a stable isotope of lead (^{206}Pb).

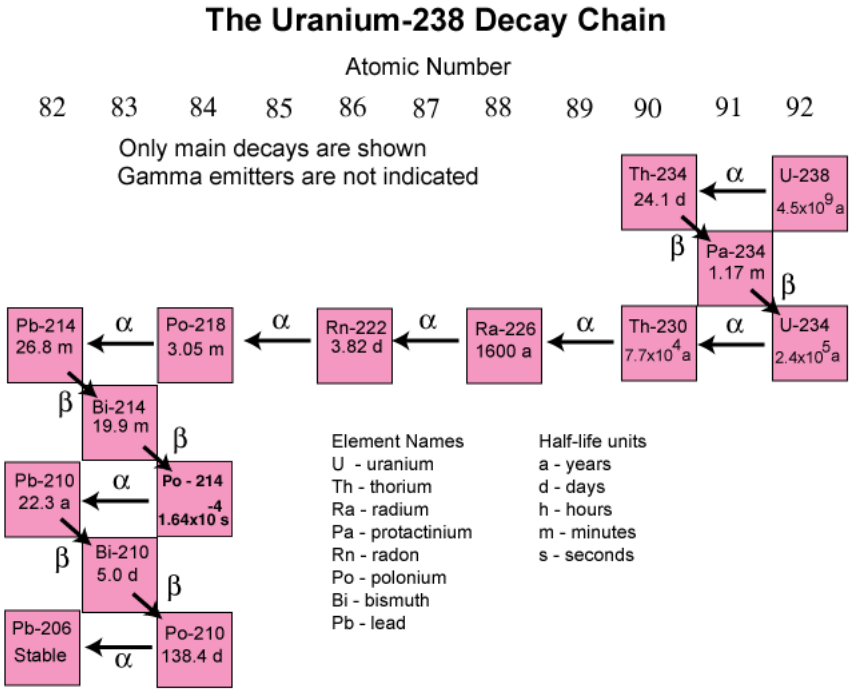

Figure 2.1: Radioactive decay series of uranium-238.

Figure 2.1 shows ^{222}Rn undergoes transformation by alpha particle emission to produce ^{218}Po, which in turn emits 6.0 MeV alpha particles with a half-life of 3.11 min to ^{214}Pb. Beta particle emissions from ^{214}Pb, with $t_{1/2}$ = 26.8 min and ^{214}Bi, with $t_{1/2}$ = 19.9 min produce ^{214}Po, which quickly ($t_{1/2}$ = 164 μs) produces the end product ^{210}Pb by emission of 7.69 MeV alpha particles. The end product ^{210}Pb is effectively stable with a half-life of 22.3 yr and is treated as such in most calculations of radon and its progeny. Properties of this important segment of the uranium series are shown in simplified form in Figure 2.1 and Table 2.2.

From radon daughters, the two that cause the most damage to human tissues are the isotopes of polonium, ^{218}Po and ^{214}Po, since both are alpha-emitting isotopes, and alpha particles can cause great damage to human tissues. In contrast, the damage imparted by beta particles is relatively minor so that they are often neglected.

Table 2.2: Radon and its radioactive products.

Element	Half-life	Principal radiation
^{222}Rn	3.82 day	α
^{218}Po	3.11 min	α
^{214}Pb	26.8 min	β, γ
^{2114}Bi	19.9 min	β, γ
^{214}Po	164 μmin	α
^{210}Pb	22.3 year	β

2.2.2 Radioactivity of Radon

Radon (^{222}Rn) is a natural radioactive gas derived from geological materials. It can easily leave the place of emission (soil, rock and building material) and enter the indoor air [14], because soil and also most earth-based building materials have $10^3 - 10^4$ times higher gas concentration gradient between such materials and open air [15]. ^{222}Rn is an alpha emitting nuclide and it is present in the air we breathe and in the water we drink [16]. On decay of ^{222} Rn, its short-lived progeny, ^{218}Po (α-particle emitter), ^{214}Pb (β-particle emitter), ^{214}Bi (β-particle emitter) and ^{214}Po (α-particle emitter) are formed. This subgroup effectively ends with ^{210}Pb, which has a half-life of 22 years. This half-life is much larger than those of radon and radon progeny. Therefore, when radon and radon progeny decay completely, the resulting activity or concentration of ^{210}Pb is very much smaller than those of the radon and radon progeny and in most cases the resulting ^{210}Pb and the remainder of the Uranium Decay Series are of no concern [17].

When radon gas is inhaled, high energy ionizing alpha particles are produced from the decay of ^{222}Rn. Each of the alpha particles can interact with biological tissue in the lungs and they cause damage to cell DNA. Such damage is the primary cause of cell death caused by radiation, because DNA contains genes (chromosomes) that hold information for cell functioning and reproduction that are critical to cell survival.

It has been shown, since the 1960, that exposure to radon and its progeny has been ranked as the second leading cause of lung cancer after smoking. The greatest fraction (55%) [18] of the natural radiation exposure in humans results from inhalation of the short-lived decay products of radon (^{222}Rn), which occur in the free atmosphere and in higher concentrations in the room air of buildings. Since 1980's, the inhaled progeny of ^{222}Rn were recognized as the most important single contributor to internal

radiation dosimetry [19].

At the moment of decay of ^{222}Rn in air, ^{218}Po is in the atomic stage, constituting the unattached (free) fraction of radon progeny. Due to an electrostatic charge, the progeny tend to attach themselves to natural aerosols in the air to form the attached fraction [20]. During inhalation, the attached or unattached radon progeny will enter the human lungs and they accumulated in the lung by filtration. Unattached particles are deposited in the respiratory tract mainly by diffusion, whereas attached particles are deposited by sedimentation and inertial impaction. Most of the unattached radon progeny is deposited in the respiratory tract, whereas 80% of the attached radon progeny are exhaled without deposition [21]. Therefore, inhalation of unattached radon progeny has been implicated in potential health risks of ambient and indoor environments, and measurements of the unattached fraction are essential for the estimation of dose.

The management of the risk of exposure related to any situation where individuals are exposed to radon and its decay products could be based on one of two approaches.

1. Epidemiological approaches

   Uses epidemiological studies and risk estimates for lung cancer derived directly from studies on cohorts of miners, taking into account any differences between the populations involved and their conditions of exposure.

2. Dosimetric approaches

   The relationship between exposure to radon progeny and dose to cells in the respiratory tract, is extremely complex and is dependent on both biological and non-biological factors. We cannot make measurement directly the dose of alpha energy delivered to target cells in the lungs, instead modelling approaches are used to simulate the sequence of events from inhalation of radon progeny to cellular injury by alpha particles [22]. Dosimetric approach uses the biokinetic and dosimetric models developed by the ICRP to calculate doses, and hence risks, which considers a range of parameters relevant to doses.

Measurement of radon concentration is a starting point for the determination of effective dose received by the local population. To determine the effective dose, it is necessary to know the DCF. The DCF is defined as the effective dose per unit exposure to radon progeny, and is traditionally given in mSv/WLM.

It is possible to find two values for DCF: Epidemiological DCF, is based on a comparison

of the detriment per unit of exposure to radon progeny derived from miner studies with the detriment per unit effective dose, which is centred between 4 and 6 mSv/WLM, and Dosimetric DCF about 15 mSv/WLM.

There are several investigations about the reduction of the discrepancy of the DCF for the radon progeny between the dosimetric and epidemiological studies had been carried out. To close the gap three radon lung dosimetry models are produced.

- RADEP/IMBA code, based on the ICRP Human Respiratory Tract Model, a deterministic regional compartment model,
- RADOS model, a deterministic airway generation model and
- IDEAL dosimetry model, a stochastic airway generation model.

For the same exposure conditions and the same physical and physiological mechanisms, currently used radon lung dosimetry models have produced different dose conversion factor (DCF) [23]. Resulting dose conversion factors ranged from 7.8 mSv/WLM (IDEAL) to 11.8 mSv/WLM (RADEP/IMBA), with 8.3 mSv/WLM (RADOS). Such dose uncertainties have significant implications for the analysis of lung cancer data in terms of dose effect relationships.

2.3 Health effects of ionizing radiation

All living matter is composed of atoms joined into molecules by electron bonds. Ionizing radiation is energetic enough to displace atomic electrons and thus break the bonds that hold a molecule together. This produces a number of chemical changes that, in the case of living cells, can lead to cell death or other harmful effects [18].

2.3.1 Chemical effects

Mammalian cells are typically $\sim$ 70-85% water, $\sim$ 10-20% proteins, $\sim$ 10% carbohydrates, and $\sim$ 2-3% lipids [24]. Water plays a central role in radiation interactions within biological systems. Let us look at what radiation does to water molecules. The symbol for water is H_2O. This means that two hydrogen atoms and one oxygen atom are bonded together to exist as one water molecule. When H_2O molecule is struck by radiation, the molecule picks up the energy lost by the radiation in the collision. If the energy gain is sufficient to overcome the bonding force holding

the molecule together, water molecules are ionized by removal of electrons, leaving positively charged molecules (H_2O^+).

$$H_2o \longrightarrow H_2o^+ + e^- \tag{2.23}$$

The released electrons combine almost instantaneously ($< 10^{-18}$sec) with neutral water molecules to form negatively charged molecules (H_2O^-). These positively and negatively charged water molecules are unstable, dissociating into ions ($H^+$and OH^-) and free radicals (denoted by a dot placed to the right of the atomic symbol) ($H^\bullet$ and $OH^\bullet$).

Free radicals in biologic specimens tend to react within 10^{-5} sec and they also react among themselves and with water, organic molecules, oxygen and their own reaction products. The products of free radical reactions include poisons such as hydrogen peroxide (H_2O_2). Of particular interest is the interaction of free radicals with oxygen, which serves to prolong the presence of free radicals.

When a free radical $H^\bullet$ interacts with molecular oxygen O_2, the product is a longer-lived free radical.

$$H^\bullet + O_2 \longrightarrow HO_2{}^\bullet \tag{2.24}$$

Thus, oxygen increases the effects of free radicals by allowing the radicals to survive long enough to migrate farther from their origin, thus expanding the potential for biologic damage [11].

2.3.2 Biological effects

All living organisms are made of cells, which themselves are made of atoms. Radiation can interact with these atoms in many different ways. At the most basic level, radiation can either ionize an atom or interact with its nucleus. In terms of biological damage, both of these interactions can have serious consequences if they result in weakening the bonds between atoms. A weak bond may eventually break up and cause the cell to malfunction [25].

The radiation safety practices are intended to minimize the dose received (energy deposited) to the body due to ionizing radiation. This is necessary because biological effects due to radiation have been observed, either directly as in the case of high, single exposures, or in some percentage of a population, as in the case of somewhat lower exposures [26]. A knowledge of these biological effects helps to assess the risks associated with exposure to radiation.

Generally, we divide the biological effects of ionizing radiation into two categories.

1. Somatic effects

   Somatic effects are effects occurring in the exposed person, that, in turn, may be divided into two temporal classes.

   a) Early or prompt effects are observable soon after a large or acute dose (dose to the whole body delivered in a short time) for example, but include the various radiation syndromes that may extend for months.

   b) Late or delayed effects, such as cancer, cataract, cardiovascular disease, and radiodermatitis may occur years after exposure to radiation [27].

2. Genetic effects

   Genetic effects are abnormalities that may occur in the future children of exposed individuals (mother or father) and in subsequent generations. If the chromosome of a cell is permanently damaged, it can lead to genetic changes. If the exposed cell is related to reproduction, damage to its DNA can lead to developmental problems in the offspring of the person. Such cell changes are generally termed as germ-line mutations and do not affect the exposed person. The hazards associated with germ-line mutations range from premature death and miscarriage to cancer in later life [25].

All biological effects produced by ionizing radiation result from the chemical events that occur shortly after the initial deposition of radiation energy.

2.4 Radiation protection quantities and units

When radiation is emitted, regardless of what type it is, it produces various interactions that deposit energy in the medium that surrounds it. This deposition of energy is characterized as radiation dose, and if it occurs in the living tissue of individuals, the endpoint effects will be biological change [5]. Understanding these interactions leads naturally to the determination of radiation exposure and dose, and the units used to define them.

Absorbed dose

The absorbed dose D_E specifies the amount of energy dE transferred by radiation per unit mass dm of a material,

$$D_E = \frac{dE}{dm} \tag{2.25}$$

The conventional unit for absorbed dose is the rad (radiation absorbed dose). The SI unit of absorbed dose is the gray (Gy) and is defined as:

$$1Gy = \frac{1J}{1kg}$$

$$1Gy = 100\,rad$$

Equivalent dose and radiation weighting factors

The absorbed dose does not contains information about the biological effects of the radiation which is determined by the ionizing efficiency along the track of the ionizing radiation in the biological tissue. To overcome this problem the definition of equivalent dose is necessary because different radiations produce different amounts of biological damage even though the deposited energy may be the same. Biological effects depend not only on the total energy deposited, but also on the way in which it is distributed along the path of the radiation. Radiation damage increases with the linear energy transfer (LET) of the radiation; thus, for the same absorbed dose, the biological damage from high-LET radiation (alpha particles) is much greater than from low-LET radiation (beta particles, gamma rays) [5]. equivalent dose H which is the absorbed dose multiplied by a quality factor Q which depends on the kind of radiation:

$$H = D_E \times Q \tag{2.26}$$

In the conventional system of units, the unit of dose equivalent is the rem (radiation equivalent man) which is calculated from the absorbed dose as:

$$rem = rad \times Q$$

Dose equivalent can also be expressed in SI unit sievert (Sv).

$$1Sv = 100\,rem$$

Quality factor, Q, also known as the weighting factor or relative biological effectiveness. It is selected from experimental values of the relative biological effectiveness (RBE), which is the ratio of X-ray dose (D_x) to dose of the test radiation (D_p) that produces the same effect:

$$RBE = \frac{D_x}{D_p}$$

It is an empirical quantity, which depends on the biological system, the observed endpoint and the conditions of the experiment. The value of Q varies with the type of radiation and their values are given in table 2.3 [28]. Since the alpha

Table 2.3: Radiation quality factors

Types of radiation	Quality factor
Gamma or X-ray	1
Beta	1
Neutrons	
<10 Kev	5
10 Kev – 100 Kev	10
100 Kev – 2 Mev	20
2 Mev – 20 Mev	10
>20 Mev	5
Proton	10
Alpha particle	20

particles possess approximately 7000 times the mass of a beta particle and twice the electronic charge, and give up their energy over a very short range (<100 μm). Alpha particles usually possess energies in the Mev range, and because they lose this energy in such a short range are biologically very efficacious, i.e. they possess a high linear energy transfer and are associated with high relative biological effectiveness [29]. Therefore the dose from the beta and gamma radiation is small in comparison, and becomes negligible when the quality factor (relative biological efficiency) of alpha irradiation is taken into account.

Considering the effects of various radiations R on a special tissue T, the equivalent dose H_T received by this tissue is:

$$H_T = \sum Q_R \cdot D_{T,R} \tag{2.27}$$

$D_{T,R}$ is the absorbed dose averaged over the tissue T due to the radiation R and the sum is taken over all radiations R [30].

Effective dose and tissue weighting factors

Radiation damage in biological tissue depends not only on the kind of radiation, but also on the kind of tissue. Different organs or parts of the human body show different sensitivities to radiation exposure [28]. This can be quantified by tissue weighting factors w_T as in table 2.4, where the effective dose H_{eff} is the sum of the equivalent doses to different tissues H_T weighted by w_T:

$$H_{eff} = \sum w_T \cdot H_T \tag{2.28}$$

Table 2.4: Tissue weighting factors for different organs

Organ/tissue	Weighting Factors
Gonad	0.2
Red Marrow, Colon, Stomach, Lung	0.12
Breast, Bladder, Oesophagus, Liver, Thyroid	0.05
Bone Surface, Skin	0.01
Remainder	0.05

2.5 Aerosols and Airborne Radon decay products

The Earth's atmosphere is a two-phase system consisting of gases and particles (solid or liquid). This means the entire atmosphere is, by definition an aerosol. Aerosol refers to suspension of liquid or solid particles in a gaseous medium and they are formed by the conversion of gases to particles or by the disintegration of liquids or solids into finer constituents [31].

When the particles are all the same in size, an aerosol is termed monodisperse. This is extremely rare in nature. Generally, particles vary in size, and this is called polydisperse. When its particles are chemically identical, an aerosol is called homogeneous. When particles are spherical, their radius or diameter can be used to describe their size. Since most particles are not spherical, however, other parameters must be used. Often the diameter is defined in terms of particle settling velocity and diffusion coefficient. All particles with similar settling velocities or diffusion coefficients are considered to be the same size, regardless of their actual size, composition or shape.

The gas radon (^{222}Rn) is emitted from the ground into the atmosphere, where it decay and form daughter products, isotopes of polonium, bismuth and lead, which either remain airborne till they decay, or are deposited by diffusion to the ground.

When a radioactive nuclide decays, electrons are stripped from the parent atom by its recoil and decay products are formed as positive ions. These ions can attract liquid and even solid material, thus forming clusters of atoms or particles in the submicron region ranging from 0.0005 to 10 μm [32].

The radon daughter aerosol in the atmosphere is generated in two steps.

1. Unattached mode: After the formation from the radon isotope by decay, the freshly generated, positively charged radionuclides react very fast (< 1 sec)

with trace gases and air vapours, and become small particles, called clusters with diameters from 0.5–5 nm and have a high mobility. The mobility is characterized by the diffusion coefficient that controls the formation of the radioactive aerosol by attachment, the deposition on surfaces and in the human lung [33].

2. Attached mode: Besides the cluster formation, these positively charged radionuclides attached to the existing aerosol particles in the atmosphere within 1-100 sec, forming the radioactive aerosol of the radon daughters.

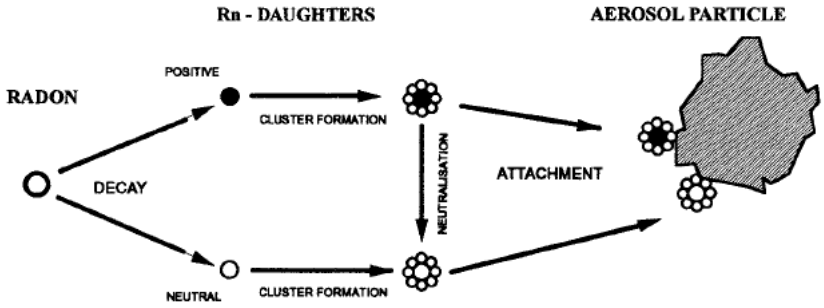

Figure 2.2: Basic processes of radon decay product behaviour in air defining unattached and attached particle activities

At height in the atmosphere, the decay products are in equilibrium with ^{222}Rn, i.e, the concentration of radon decreases with height, but near the ground this is not observed, because Some of the radon has been exhaled too recently for equilibrium to have been reached. Also, decay products, being isotopes of elements which are solids at normal temperatures, deposit on the ground.

There is higher concentration of radon in indoors than outdoors (home environment) [16] because of:
(i) Air movement is less.
(ii) Radon is exhaled from walls as well as from the floor.
(iii) Slight negative pressures indoors, caused by heating and by effects of wind, draw in air from the soil below.

The largest proportion of the natural radiation dose to human results from the inhalation of the short-lived radon decay products ^{218}Po, ^{214}Pb, ^{214}Bi and ^{214}Po. In the atmosphere, radon progeny diffuses and mixes with air.

While breathing, inhaled aerosols (attached or unattached radon progeny) can be deposited and transformed in respiratory tract. The particles that are emitted

during radioactive decay are emitted with a certain energy and they may or may not have charge. All of them interact with the respiratory tract, transferring energy and eventually dissipating all of their energy [34].

2.6 Health Effects of Radon

The health effects of exposure to radon are caused primarily by damage due to alpha particles. It is generally accepted that alpha particles have the potential to inflict 20 times the biological damage on tissues as beta particles and gamma rays of the same energy. The most important health risk associated with radon and its progeny is lung cancer.

2.6.1 Units for measuring radon

When radon and radon progeny are inhaled, the resulting radiation dose to the lung is primarily due to the radon progeny and not to radon itself and the dose to the lung is primarily from the emissions of α-particles, with the β-particles and γ-rays contributing a small percentage of the total dose. Finally, significant fractions of the radon progeny that are inhaled are retained in the lung and, due to their short half-lives, they decay before they can be cleared from the lung.

The units described in this section for application to radon and its progeny involve measurement of the rate of radioactive decay and the amount of energy released.

Activity

In general, the activity of a sample is a measurement of the rate of decay of that sample. The SI derived unit of activity is called the Becquerel and the unit symbol is Bq. The activity concentration units are Bq m^{-3}. The old unit of activity is curie (Ci).

One Ci is approximately equal to the activity of 1 gram of ^{226}Ra, which is equal to 3.7×10^{10} disintegrations per second. Thus,

$$1Ci = 3.7 \times 10^{10} Bq, \tag{2.29}$$

Potential alpha energy concentration

The potential alpha energy concentration (PAEC) is the sum of all the potential alpha energy in unit volume of air if all the radon daughters decay to ^{210}Pb, and is

a measure of the potential dose if the solid products are deposited in the respiratory tract. A common unit for this quantity is Jm^{-3} and $1WL = 20.8\,\mu Jm^{-3}$. The PAEC can be calculated from the individual radon progeny concentrations by the following equation:

$$PAEC(\mu Jm^{-3}) = 0.000578C_1 + 0.00285C_2 + 0.00210C_3, \tag{2.30}$$

where C_1, C_2, and C_3 are the concentrations of ^{218}Po, ^{214}Pb, and ^{214}Bi, respectively (Bqm^{-3}).

$$PAEC(WL) = 0.00103C_1 + 0.00507C_2 + 0.00373C_3 \tag{2.31}$$

where C_1, C_2, and C_3 are the concentrations of ^{218}Po, ^{214}Pb, and ^{214}Bi, respectively ($pCiL^{-1}$).

Equilibrium equivalent concentration

The equilibrium equivalent concentration, EEC, is defined as the activity concentration of radon that would result if the radon progeny were in secular equilibrium with the radon and have the same PAEC as the non-equilibrium mixture to which the EEC refers. This quantity is expressed in the unit Bqm^{-3} or $pCiL^{-1}$. The EEC can be derived from the individual concentrations of the radon progeny using the following formula:

$$ECC = 0.105C_1 + 0.516C_2 + 0.379C_3, \tag{2.32}$$

In indoor air, the equivalent concentration is often about half the actual radon concentration. High in the atmosphere, the equivalent and actual radon concentrations are the same [16].

Equilibrium factor

The equilibrium factor, F, is defined as the ratio of the total potential alpha energy for the actual progeny concentrations to the total potential alpha energy of the progeny which would be found if the progeny were in equilibrium with the parent gas [35]. Thus

$$F = \frac{ECC}{C_0}, \tag{2.33}$$

The concentration of each of the radon progeny can be expressed as a fraction of the concentration of radon;

$$F_i = \frac{C_i}{C_0}, \tag{2.34}$$

The equilibrium factor equation (2.33) can be calculated from the following:

$$F = 0.105F_1 + 0.516F_2 + 0.379F_3, \tag{2.35}$$

Working level

The Working level (WL) unit is defined as any combination of the short-lived decay products of radon in 1L of air that will result in the ultimate emission of $1.3 \times 10^5 MeV$ or $2.08 \times 10^{-5} jm^{-3}$ of α-particle energy, which is widely used to describe the potential alpha energy concentration of radon progeny. This would mean $100 pCiL^{-1}$ or $3700 Bqm^{-3}$ of each of ^{222}Rn, ^{218}Po, ^{214}Pb, ^{214}Bi, and ^{214}Po [17].

The working level is a measure of exposure rate. It describes how much energy is found in the alpha particles in a litre of air. In order to relate this energy to biological deposition and absorbed dose, many additional factors must be considered. These include the breathing rate, the volume of air per breath, the time the radon progeny remain in the body, and the half-lives of the progeny.

Working level month

The Working Level Month (WLM) is defined as exposure to decay products equivalent to 1 WL for 170 h, this being the nominal number of hours worked per month in a mine. It is still used in discussions of the epidemiology of lung cancer in relation to exposure to radon and its decay products [16].

Potential alpha energy exposure

The dose from radon progeny can be related to the potential alpha energy exposure. The potential alpha energy exposure (E) is the time integral over the potential alpha energy concentration of the progeny mixture to which the individual is exposed for a time T:

$$E = \int_o^T C_p(t) dt, \tag{2.36}$$

When the potential alpha energy concentration C_p is a constant, $E = C_p T$ where T is the time involved.

The traditional unit of potential alpha energy exposure is the Working Level Month (WLM). The potential alpha energy exposure in WLM is calculated by multiplying the PAEC in WL by the number of hours worked in an environment with that value of PAEC and dividing by 170 working hours per month. The SI unit for potential α-energy exposure is Jhm^{-3}.

$$1 WLM = 170h \times WL = 2.2 \times 10^7 MeVhL^{-1} = 3.5 \times 10^{-3} Jhm^{-3}, \tag{2.37}$$

There are 51.6 periods of 170 h in a year. Thus an annual exposure to 1 WL would correspond to 51.6 WLM.

2.7 The Respiratory System and its Exposure to Radon

The respiratory tract consists of four anatomical regions. Figure 2.3 provides a schematic representation of the human respiratory system.

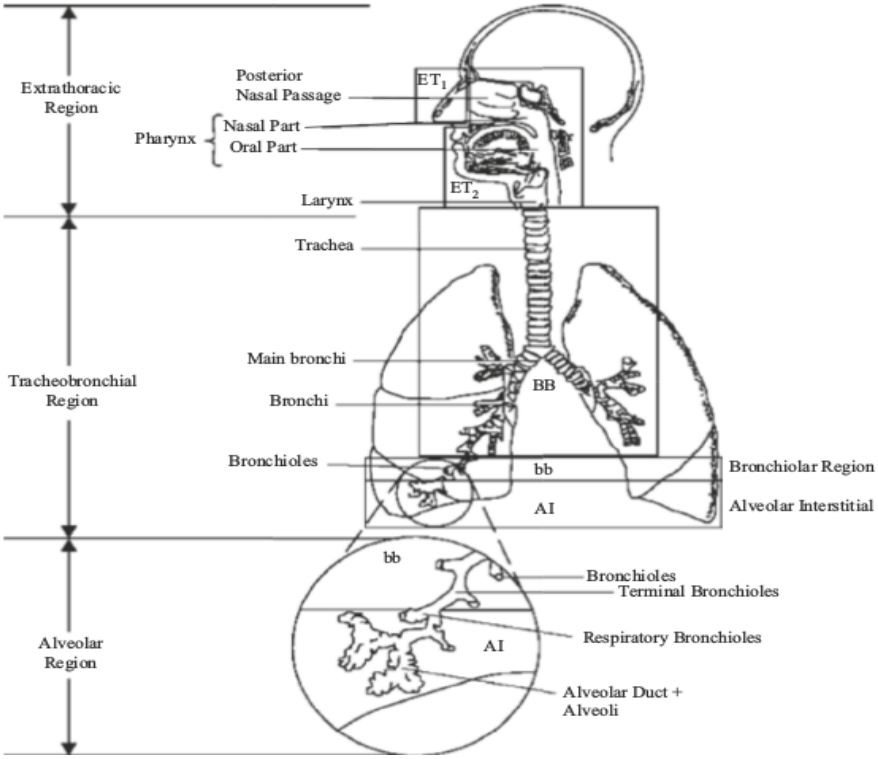

Figure 2.3: Morphological overview of the human respiratory tract.

Extrathoracic Region (ET) Which consists of the anterior nose (ET_1) and the posterior nasal passages, larynx, pharynx and mouth (ET_2).

The main task of this region is to condition and clean the inspired air and conduct it to the trachea and the lungs. Ambient air, which is usually of lower temperature and humidity than the human body, is efficiently modified before penetrating deeply into the lungs.

The Bronchial Region (BB) Consisting of the trachea and bronchi, from generation[1] 0 (trachea) up to generation 8. This region is the most interesting one for radiation protection considerations because the majority of lung cancer originates in this part of the respiratory tract [20]. The BB region includes the trachea

[1]Position of airways in lung relative to the trachea.

(generation 0), bronchi (generation 1–8). The purpose of this part of the airway tree is to conduct air. It adjusts the humidity and temperature of inspired air and is the site of the deposition of inhaled particles by impaction, sedimentation, and diffusion.

The Bronchiolar Region (bb) This region consists of airway tubes between generations 9 and 15. The last generation (15) is called terminal bronchioles.

Alveolar-Interstitial Region (AI) This region sometimes called the pulmonary region., which starts from the terminal bronchioles and includes generations 16–23. The main function of this region is to exchange gases, although other roles are also important. Inhaled particles reaching this region are deposited by sedimentation or diffusion.

There are about 5×10^8 alveoli, each on average about 150 μm in diameter. The walls of the extrathoracic and tracheobronchial (trachea, bronchi and bronchioles) regions are covered with cilia, which propel the mucous layer out of the respiratory tract. Particles caught in the mucous are brought up and eventually swallowed. The alveoli are not ciliated, and particles deposited in the pulmonary region remain there until they dissolve in lung fluid, or are engulfed by wandering cells called macrophages, which transport them to the ciliated bronchioles or to the lymphatic system of the lung [32].

2.7.1 Respiratory physiology

Radiation doses to tissues and cells of the respiratory tract from the inhalation of radioactive particles and gases are determined to a great extent by physiological parameters [36]. These parameters vary slightly among different populations in the world and among individual members of these populations.

The physiological parameters relevant for the dosimetric model are: Total lung capacity: is volume of air in the lung at maximum inhalation, Functional residual capacity: is the volume of air left in the lung after normal exhalation, Dead space: is the volume of the conducting airways in which no gas exchange takes place, Tidal volume: is volume of air inhaled per one breath, Breathing rate: is volume of air inhaled per unit time (m^3/h) and Breathing frequency: is number of breath per minute .

2.7.2 Mechanisms of aerosol deposition

Particle deposition in the respiratory tract is determined by three different mechanisms, which move particles out of the streams of inhaled and exhaled air toward the airway walls.

1. **Inertial impaction**: occurs when airborne particles possess enough momentum (product of mass and velocity) to keep its trajectory despite changes in direction of the air stream, consequently colliding with the walls of the respiratory tract.

   Inertia is the inherent property of a moving mass to resist accelerations. It may cause particles to continue to move in their original direction and not follow airflow streamlines, such that they deposit on airway walls by impaction. Inertial impaction will most likely occur in the extrathoracic airways and in the large conducting airways of the lung, where flow velocities are high and rapid changes in airflow direction occur.

2. **Sedimentation**: is a time-dependent process in which particles are continually exposed to gravity and undergo gravitational settling. The distance a particle settles within a given time increases with its mass. The longer a particle remains in the respiratory system, the larger is the settling distance the particle will cover and their is high probability that the particle will touch airspace walls. Therefore, the relative long residence time in the small conducting airways and in the gas-exchanging region of the lung will favour particle deposition by gravitational sedimentation.

3. **Diffusion**: occurs when particles are sufficiently small to undergo a random motion due to molecular bombardment. This process, also known as Brownian motion. Collisions between gas molecules and a particle cause numerous very small random displacements of that particle. The distance a particle will travel by diffusion increases with time and with decreasing particle diameter. Hence, the probability of particles to hit airspace surfaces by diffusional transport is larger the smaller the particles are and the longer they remain in the respiratory system. Consequently, the lung periphery with its small airway dimensions favors deposition by diffusion. Residence time is long, and the distance a particle has to travel before it hits an airspace wall is short [37].

Particles with diameters much greater than the mean free path of the surrounding gas are said to be in the 'continuum' regime where their surfaces are constantly being impacted by air molecules from all directions. In contrast, particles whose diameters are smaller than the mean free path of the air are said to be in the 'free-molecular' regime where the impact by air molecules is intermittent and the effect of being struck by a moving air molecule overwhelms the effects of gravity on the particle [17].

With decreasing particle diameter, diffusional particle displacement increases so that particle deposition in the respiratory system increases. With increasing particle diameter, the distance covered by sedimentation or impaction increases such that total particle deposition is also enhanced.

2.7.3 The ICRP deposition Model

One of the most widely used and highly regarded bases for dosimetric calculations associated with inhalation of radioactive materials is the HRTM of the ICRP.

ICRP is an independent, international, non-governmental organization, with the mission to provide recommendations and guidance on radiation protection. The respiratory tract is an important route for radionuclides and other hazardous airborne materials to enter the body. Inhaled radionuclides irradiate tissues and cells of the respiratory tract as well as those of many other organs [38].

Deposition of inhaled aerosols refers to the initial processes determining how much of the material in the inspired air remains behind after expiration. In a mathematical sense, it refers to the mean probability for an inspired particle to be caught in the respiratory system. Deposition occurs when particles strike the wet airspace surfaces of the respiratory tract, the site of initial particle contact with the airspace surface is considered the site of initial deposition [37]. It is one of the most important issues in the human respiratory tract model. The aerosols are mixed in air and they enter into the human lung during inhalation. A fraction of them is deposited in the lung while the rest is ejected from the body during exhalation.

Deposition behaviour of aerosols in the respiratory tract is required to estimate the fractions of radioactivity in breathing air that are deposited in each anatomical region of exposed individuals and it occurs during both inspiration and expiration. Deposition occurs in all compartments of the human lung, but with different efficiencies.

Deposition efficiency (DE) is defined as the ratio of the deposited particles in a region to the total number entering nasal cavity. That is

$$DE = \frac{\text{deposited particles}}{\text{particles entering the nasal cavity}}, \tag{2.38}$$

Deposition fraction refers to the concentration of particles in the aerosol that has inhaled through nose or mouth deposited in respiratory tract.

There are two groups of deposition processes, i.e., thermodynamic (for small particles) and aerodynamic (for larger particles) deposition.

The behaviour of small size particles (which are deposited by diffusion) is described in terms of the thermodynamic diameter (d_{th}) and the diffusion coefficient D. Deposition of larger particles is described by the aerodynamic diameter d_{ae}. The aerodynamic diameter is defined in terms of the equivalent particle diameter d_e [2] by the following formula:

$$d_{ae} = d_e \sqrt{\frac{\rho C(d_e)}{\chi \rho_0 C(d_{ae})}}, \tag{2.39}$$

where ρ is the particle density, $\rho_0 = 1 g cm^{-3}$ (unit density), χ the particle shape factor and C is the so-called Cunningham correction slip factor [3].

The thermodynamic diameter is given in terms of its aerodynamic diameter by the following equation:

$$d_{th} = d_{ae} \sqrt{\frac{\chi \rho_0 C(d_{ae})}{\rho C(d_{th})}} \tag{2.40}$$

In ICRP66 deposition model a semi-empirical approach has been used to describe the regional deposition. Relative simple algebraic equations derived from experiments and theory are used for the deposition model. The filtration efficiency (deposition efficiency) for an anatomical region is given in the form:

$$\eta = 1 - e^{-aR^p} \tag{2.41}$$

where a and p are parameters and R is a function of the particle diameter and flow rate. It is given separately for thermodynamic and aerodynamic depositions.

If both kinds of deposition processes (thermodynamic and aerodynamic) are present, the combined effect is given as a quadratic sum:

$$\eta = \sqrt{\eta_{th}^2 + \eta_{ae}^2} \tag{2.42}$$

[2] diameter of a spherical particle with the same volume as the considered particle.

[3] Used to account for non-continuum effects when calculating drag force on small particle and become significant for particles smaller than $15 \mu m$.

where η is the total deposited fraction, while η_{th} and η_{ae} are the thermodynamic and aerodynamic deposition fractions.

For particles with thermodynamic diameters smaller than 5 nm, diffusion deposition is dominant [39]. If the aerodynamic diameter is larger than 10 nm, aerodynamic deposition is the most important [40].

The respiratory tract can be considered as a series of three filtering units: the extrathoracic region (ET, including the nose, mouth, pharynx, and larynx), the bronchial (BB) and bronchiolar (bb) conducting airways (including trachea), and the alveolar interstitial (AI) region [41].

During inhalation, smaller and smaller fractions of the tidal volume pass through the filters in turn, which are determined by the cumulative volumes of the preceding filters. During exhalation, the same volume of air passes through the same filters as those during the inhalation [42]

The fraction of the number of inhaled particles deposited in the whole respiratory tract is referred to as total deposition. The fraction of the number of inhaled particles deposited in a single region of the respiratory tract is referred to as regional deposition. The total deposition is therefore the sum of the regional deposition values.

CHAPTER 3
Mathematical Model

The empirical ICRP respiratory tract dosimetry model was developed by the International Commission on Radiological Protection. This model can be used to estimate regional deposition in the lungs as a function of particle characteristics and ventilatory conditions via a number of algebraic equations [38].

A home written Fortran computer program has been developed to perform calculation for the regional deposition for unattached radon progeny that follows ICRP66 recommendations, which consists of the following steps.

3.1 Input of data

Some input parameters for unattached radon decay products were required before running the program, which included

1. Density;
2. Breathing rate;
3. Breathing frequency;
4. Functional residual capacity (FRC);
5. Shape factor: defined as the ratio of the resistive force of irregular particle to that of spherical particle with the same volume and velocity;
6. Hygroscopic growth factor: is the tendency of a solid substances to absorb moisture from the surrounding atmosphere;
7. Dead spaces in ET, BB, bb regions.

In present consideration, all calculations for the unattached progeny have been performed with the best estimates of inputs for a home environment which are given by [40] as in table 3.1.

According to table 3.1, the particle density for unattached mode particles was 1 g/cm^3; the particle shape factor for the unattached mode particles was 1; the hygroscopic growth factor for the unattached mode particles was 1.

Table 3.1: Best estimates of unattached aerosol parameter values for home conditions.

Parameter	Best estimate	Parameter value range
Unattached fraction	8%	0–50%
Aerosol size	0.9 nm	0.5–3.5 nm
Hygroscopic growth factor	1	1–2
Equilibrium factor	0.4	0.1–1
Particle density	1 g/cm^3	1–2 g/cm^3
Shape factor	1	1-1.9
Breathing rate	0.78m^3/h	0.45–1.5 m^3/h
aerosol dispersion	1.3	1–1.4

The breathing rate taken to be that for a Caucasian male was 0.78 m^3/hr and the corresponding respiratory frequency was 15 min^{-1}. According to [38], the FRC for Caucasian men was define as 3300 mL and the dead spaces in ET, BB and bb regions was defined as 50, 49, 47 mL respectively, as in table 3.2.

Table 3.2: Values of anatomical and physiological parameters for adult Caucasian male.

Parameter	subject (adult Caucasian male)
FRC (ml)	3300
V_D (ET) (ml)	50
V_D (BB) (ml)	49
V_D (bb) (ml)	47
V_D (total) (ml)	146
Height (cm)	176
SF_t	1
SF_b	1
SF_A	1

3.2 Transit time of air and volumetric fractions

The time spent by a particle travelling through a section of airway is called transit time. The deposition efficiencies depend explicitly on the average transit time of inhaled and exhaled air though each region.

The transit time of air in BB (t_B), bb (t_b), AI (t_A) regions are:

$$t_B = \frac{V_D(BB)}{\dot{V}}\left(1+\frac{0.5V_T}{FRC}\right) \tag{3.1}$$

$$t_b = \frac{V_D(bb)}{\dot{V}}\left(1+\frac{0.5V_T}{FRC}\right) \tag{3.2}$$

$$t_A = \frac{V_T - V_D(ET) - [V_D(BB)+V_D(bb)]}{\dot{V}}\left(1+\frac{V_T}{FRC}\right), \tag{3.3}$$

where $V_D(ET)$, $V_D(BB)$ and $V_D(bb)$ are the dead spaces in ET, BB and bb respectively, $\dot{V}$ is the total volumetric flow rate of the air ventilating the lung, and V_T is the tidal volume (amount of air breathed in or out during normal respiration).

The algebraic expressions for the volumetric fractions in BB, bb and AI are given as:

$$V_F(BB) = 1 - \frac{V_D(ET)}{V_T} \tag{3.4}$$

$$V_F(bb) = 1 - \frac{[V_D(ET)+V'_D(BB)]}{V_T} \tag{3.5}$$

$$V_F(AI) = 1 - \frac{[V_D(ET)+V'_D(BB)+V'_D(bb)]}{V_T}, \tag{3.6}$$

and

$$V'_D(BB) = V_D(BB)\times\left(1+\frac{V_T}{FRC}\right)$$

$$V'_D(bb) = V_D(bb)\times\left(1+\frac{V_T}{FRC}\right),$$

where $V_F(BB)$, $V_F(bb)$, and $V_F(AI)$ are volumetric fractions in BB, bb and AI respectively.

The ICRP66 model takes into account the division of inspired air between the nose and mouth for mouth breathers and normal nose breathers. For normal nose breathers, 100% of inspired air goes through the nose at all physical activity levels except heavy exercise at which inspired air splits evenly between the nose and mouth as in table 3.3.

3.3 Deposition of monodispersed aerosols

If all particles of an aerosol are of uniform size, an aerosol is termed mono-disperse. In reality perfect monodispersity does not exist, an aerosol is termed mono-disperse if the aerosol dispersion was smaller than 1.2 [37].

ICRP66 recommends a set of algebraic expressions, which give reliable estimates of regional deposition efficiencies in ET1, ET2, BB, bb and AI regions. These

Table 3.3: Fraction of total ventilatory airflow passing through nose for normal nose breather

Level of exertion	Normal nose breather
Sleep	1.0
Rest	1.0
Light exercise	1.0
Heavy exercise	0.5

expressions are given in table 3.4 and have been used for the calculation of deposition efficiencies and deposited fraction in different regions of the respiratory tract for mono-dispersed particles.

The expressions for deposition efficiencies by thermodynamic (η_{th}) processes in each region have the general form:

$$\eta_{th} = 1 - e^{-aR^p}, \tag{3.7}$$

As can been seen from equation (3.7), the deposition efficiencies by thermodynamic process is expressed in terms of three parameters, namely, a, R and p. The coefficients have been derived by combining empirical analysis with the theoretical model on the basis of the mathematical formalism to experimental data and their values are listed in table 3.4 for different region of respiratory tract.

Table 3.4: Recommended algebraic expression of thermodynamic deposition for inhalation and exhalation through nose

Filter	Region	Thermodynamic regional deposition $\eta_{th} = 1 - e^{-aR^p}$		
		a	R	p
1	ET_1	18	$D(\dot{V}_n \times SF_t)^{-0.25}$	0.5
2	ET_2	15.1	$D(\dot{V}_n \times SF_t)^{-0.25}$	0.538
3	BB	22.02 $SF_t^{1.24}\psi_{th}$	D t_B	0.6391
4	bb	-76.8 + 167 $SF_b^{0.65}$	D t_b	0.5676
5	AI	170 + 103 $SF_A^{2.13}$	D t_A	0.6101
6	bb	-76.8 + 167 $SF_b^{0.65}$	D t_b	0.5676
7	BB	22.02 $SF_t^{1.24}\psi_{th}$	D t_B	0.6391
8	ET_1	15.1	$D(\dot{V}_n \times SF_t)^{-0.25}$	0.538
9	ET_2	18	$D(\dot{V}_n \times SF_t)^{-0.25}$	0.5

SF are scaling factors from a Caucasian adult male to some other subjects. A scaling factor is defined as the ratio of a reference airway size in an adult Caucasian

male to that in the subject.

3.3.1 Deposition efficiencies in extrathoracic regions

The deposition efficiencies η_{th} for nasal (ET_1) and mouth (ET_2) breathing for thermodynamic deposition were given by:

$$\eta_{th}(ET_1) = 0.5(1 - e^{-aR^p}) \tag{3.8}$$

$$\eta_{th}(ET_2) = 1 - e^{-aR^p} \tag{3.9}$$

where the constants for $\mathbf{ET_1}$, $a = 18$ and $p = 0.5$ and $\mathbf{ET_2}$, $a = 15.1$ and $p = 0.538$. R for regions $\mathbf{ET_1}$ and $\mathbf{ET_2}$ was expressed as $R = D(\dot{V}_n)^{-1/4}$, where D was the particle diffusion coefficient and $\dot{V}_n$ was the average volumetric flow rate for inhalation and exhalation through the nose in cm^3/sec.

The particle diffusion coefficient (D) which is the mean square displacement of a particle by Brownian motion per unit time ($cm^2 s^{-1}$) is:

$$D = \frac{kTC}{3\pi\mu d_p} \tag{3.10}$$

where k is the Boltzmann constant, T is the absolute temperature, d_p is the particle diameter, μ is the dynamic viscosity air [1], and C is the Cunningham slip factor.

The Cunningham slip factor is:

$$C = 1 + \frac{\Lambda}{d_p}\left\{2.514 + 0.800\exp\left[-0.55\left(\frac{d_p}{\Lambda}\right)\right]\right\}, \tag{3.11}$$

where Λ is the mean free path [2]. of air molecules at 37 ^{0}C, 99.5 % relative humidity and 76 cm Hg atmospheric pressure.

3.3.2 Deposition efficiencies in thoracic regions

The deposition in the airway tubes is considered both for inhalation and exhalation. The deposition efficiencies for BB, bb and AI regions were calculated by using the equation (3.7).

According to ICRP66, the deposition efficiency η_{th}

1. For the BB region, the thermodynamic deposition efficiency was

$$\eta_{th}(BB) = 1 - exp[-(22.02\psi_{th})(Dt_B)^p] \tag{3.12}$$

[1] A measure of the friction that is present when adjacent layers of the gas are moving with different velocities

[2] Average distance a molecule travels in a gas between collisions with other molecules

where $\eta_{th}(BB)$ was the thermodynamic deposition efficiency for the BB region, D was the particle diffusion coefficient, t_B was the transit time of air in BB region, the constant $p = 0.6391$, ψ_{th} was an empirical correction factor to allow for the enhancement of the modelled thermodynamic deposition efficiency of the bronchi caused by non-laminar bronchial airflow and

$$\psi_{th} = 1 + 100exp\left\{ - \left[\log_{10}\left(100 + \frac{10}{(d_{th})^{0.9}}\right)\right]^2 \right\}, \tag{3.13}$$

where d_{th} is particle thermodynamic diameter and given by:

$$d_{th} = d_p[1 + 3exp(-2.2 \times 10^3 \times d_p)], \tag{3.14}$$

where d_p is particle diameter in nm.

2. For the bb region, the thermodynamic deposition efficiency was

$$\eta_{th}(bb) = 1 - exp[-a(Dt_b)^p] \tag{3.15}$$

where $\eta_{th}(bb)$ was the thermodynamic deposition efficiency for the bb region, D was the particle diffusion coefficient, t_b was the transit time of air in bb region. The parameters $a = 90.2$ and $p = 0.5676$.

3. For the AI region, the thermodynamic deposition efficiency was

$$\eta_{th}(AI) = 1 - exp[-a(Dt_A)^p] \tag{3.16}$$

where $\eta_{th}(AI)$ was the thermodynamic deposition efficiency for the AI region, D was the particle diffusion coefficient, t_A was the transit time of air in AI region. The parameters $a = 273$ and $p = 0.6101$.

According to ICRP66 model, each region of the respiratory tract is represented by particle filter that acts in series, as shown in figure 3.1. Upon inhalation, air flows through ET_1, followed by ET_2, then BB, then bb, then AI. Particulates may be deposited in any of the regions or remain in the inhaled air. They then have another chance at deposition in each of the regions as the air is exhaled.

Inhalability is the ability of airborne particles are to be inspired into the respiratory tract from the environment.

After obtaining the deposition efficiencies in regions ET_1, ET_2, BB, bb and AI, the deposited fraction in those regions as a function of particle diameter during inhalation and exhalation can be calculated.

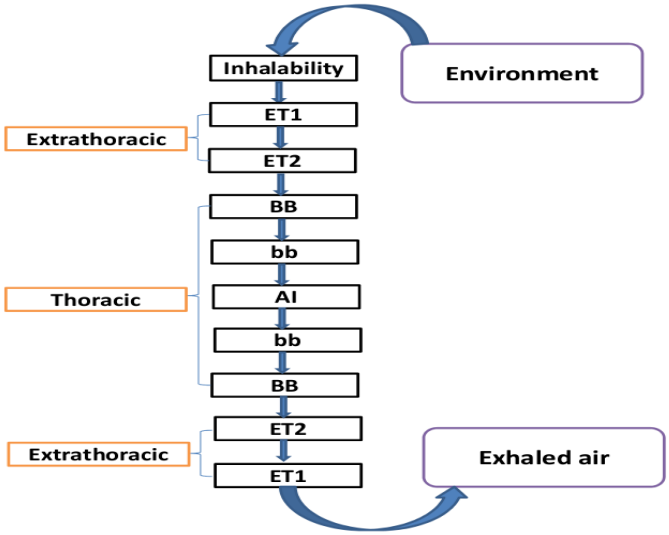

Figure 3.1: Emperical representation of inhalability of particles and their deposition in the respiratory tract during continuous cyclic breathing by transport through a series of filters.

Calculation of the deposition efficiencies in ET_1, ET_2, BB, bb and AI can be considered as a loop. The starting point of this loop is the minimal particle diameter, which is 0.5 nm. The loop will be finished when the particle thermodynamic diameter is less than or equal to the maximal particle diameter, which is 5 nm in our case. This recursive relationship is used to evaluate fractional deposition in each region of the respiratory tract for both inhalation and exhalation.

CHAPTER 4

Results and Discussions

The air around us is full of aerosol containing radon. With each breath we take, aerosol enter the nose and mouth. Aerosol may deposit at any point along their pathway by inertial impaction , sedimentation or diffusion. For evaluating the dose to the respiratory tract from inhaled particle, it is important to know where and how much the particles deposit.

The main goal of this study was to determine the deposition fraction of unattached radon progeny in human respiratory tract . Fractional deposition in each region of the respiratory tract was calculated for unattached fraction for normal nose breather adult Caucasian male. Based on the best estimates of monodispersed aerosol parameters for home conditions, the regional deposition fraction for unattached radon progeny was estimated.

A breathing rate of 0.78 m^3h^{-1}, shape factor 1, particle density 1 g/cm^3, hygroscopic growth factor 1, was adopted as a reference value for the home environment. According to Marsh and Birchall, aerosol size is in the range of 0.5–3.5 nm. In our case, we used the range 0.5–5 nm, because there is no agreement on the upper limit unattached radon progeny, however most of the literature uses 5 nm as an upper limit [43].

Errata for ICRP publication 66 was used in our calculation for dynamic viscosity of air 1.88×10^{-4} poise[1] and the mean free path of the air molecules 0.0683 μm.

Diffusion is the only an effective deposition mechanism for the deposition unattached radon progeny in respiratory tract, the rate of diffusion is proportional to the diffusion coefficient, and has inverse relation with particle size. It is 0.07 cm^2/sec for 0.9 nm, and ranged from 0.22 cm^2/sec–0.22 mm^2/sec for 0.5–5 nm.

During inhalation, air flows from regions of high pressure to regions of lower pressure from one end to the other. This flow may be laminar, where the movement

[1] $1\,poise = 0.1\,kg/m.sec$

is orderly and turbulent, where movement is chaotic.

According to ICRP66 recommendation, flow in the respiratory system can be considered laminar for thoracic and turbulent for extrathoracic region .

4.1 Deposition in extrathoracic region

On extrathoracic region, the deposition fraction for 0.5 nm particle diameters of inhaled unattached progeny are 49.03% and 48.29% for nose and mouth respectively, whereas for 5 nm particle diameter, the deposition fraction are 16.7% for nose and 19% for mouth. The extrathoracic deposition fraction decreased as particle size increased from 0.5–5 nm both for nose and mouth as in figure 4.1.

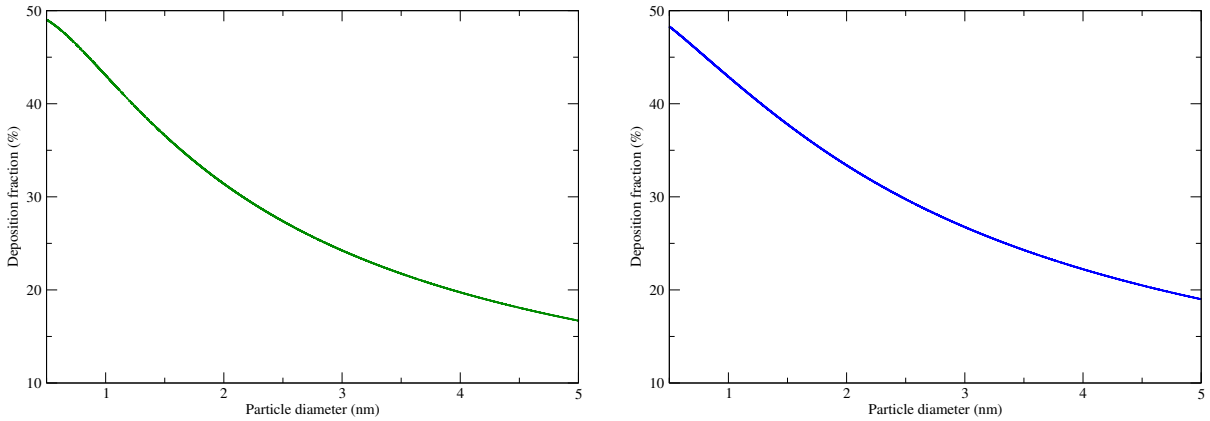

(a) nose **(b)** mouth

Figure 4.1: Deposition fraction in extrathoracic region.

Adult humans have hair in the interior nasal passage which filter foreign particles from entering the nasal cavity. The surfaces are covered by mucus, most of which is propelled by the beating of the cilia toward gastrointestinal (GI).

Since deposition efficiency depends mainly on diffusion coefficient and volumetric flow rate. For 0.78 m^3/h breathing rate, the volumetric flow rate is 433.33 cm^3/sec. Because of high diffusion coefficients and turbulent deposition flow, unattached particles also have high deposition rates in head airways.

According to ICRP66, all deposited particle in ET_1 is cleared by nose wiping, blowing, sneezing, whereas in ET_2 clearance is modelled as mucociliary action and swallowed to gastrointestinal tract. The ET_1 and ET_2 clearance rates are 1 and 100 per day.

4.2 Deposition fraction in thoracic region

On trathoracic region, the deposition fractions for 0.5 nm are 2.25%, 0.38%, 0.04% and for 5 nm 7.17%, 32.04%, 23.40% for bronchial, bronchiolar and alveolar region respectively as shown in figure 4.2.

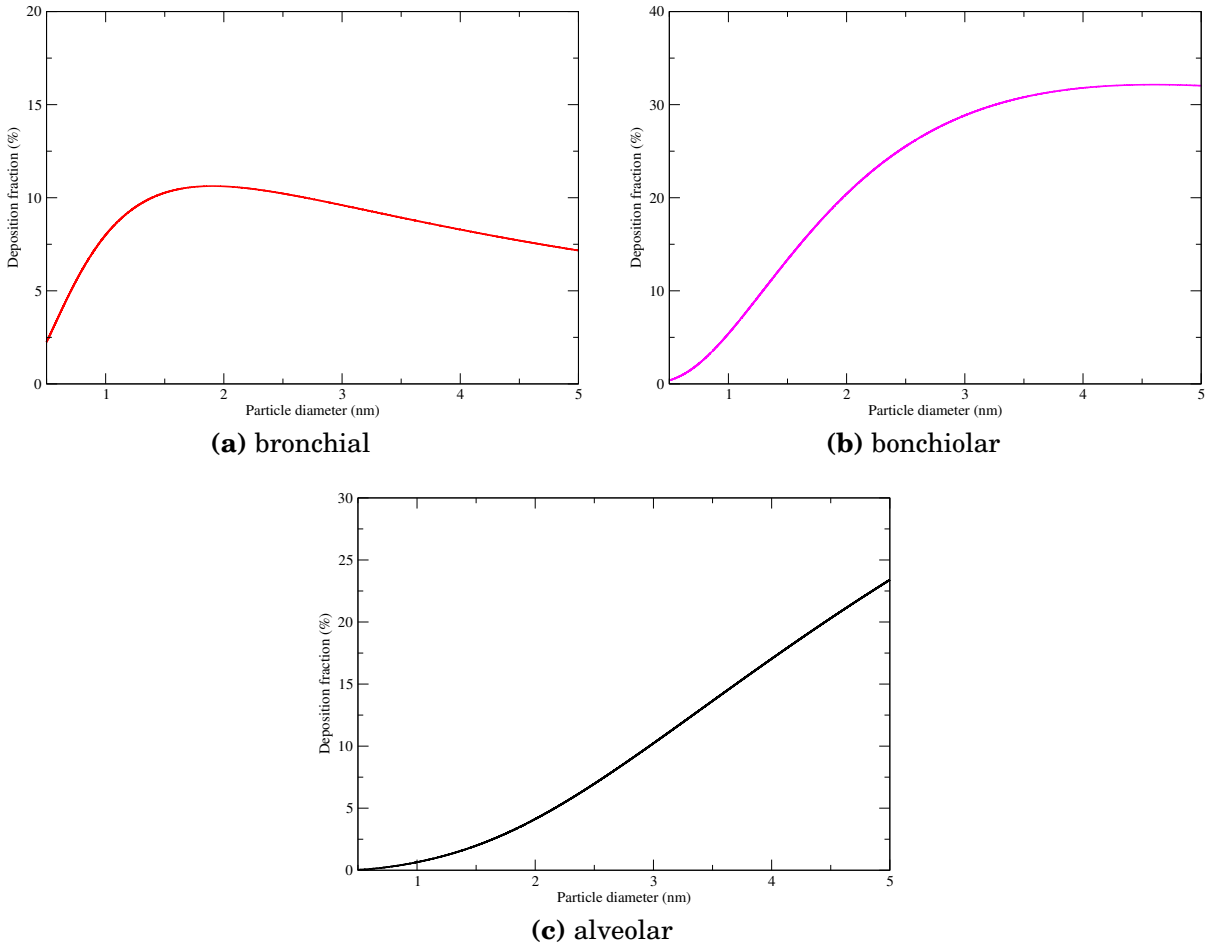

(a) bronchial

(b) bonchiolar

(c) alveolar

Figure 4.2: Deposition fraction in thoracic region.

The deposition efficiency in the thoracic region depends on diffusion coefficient and the transit time of air in that region. The transit time of air is 0.128 sec, 0.123 sec and 1.065 sec in bronchial, bronchiolar and alveolar region respectively. A laminar deposition flow in the thoracic airways was assumed.

As can be seen from figure 4.2a, the bronchial deposition fraction increased as particle size increased from 0.5 to 1.7 nm, it is constant from 1.7 to 2 nm and decreased consistently thereafter until particle diameter reached 5 nm. Increasing from 0.5–1.7 nm is due to deposition from inhalation, from 1.7–2 nm deposition from inhalation and exhalation almost equal, and the decrease from 2–5 nm is deposition from exhalation. Deposition due to inhalation is less than the deposition

due to exhalation because of the sequential nature of the regions, i.e, during inhalation, the particles that pass through bronchial, deposit in the bronchiolar and alveolar region, and back again to bronchiolar and the to bronchial with less aerosol concentration at the exhalation.

In bronchiolar, deposition fraction increased as a particle size increased from 0.5–4 nm, and constant deposition from 4–5 nm particle size 4.2b.

As can be seen from figure 4.2c, In alveolar region the deposition fraction increases as particle size increases. This is due to the decrease in diffusion coefficient of unattached radon daughters. As a result, there is low deposition fraction in upper airway and most inhaled aerosol concentration reached alveolar. Because of low flow rate, long residence time and small airway dimensions, deposition increases as particle diameter increases for unattached aerosol range.

Particles deposited in tracheobronchial regions are eliminated, in minutes to hours, by cilia propelled mucus flow. Particles deposited in the pulmonary region may be phagocytized by alveolar macrophages. Macrophages with engulfed particles may then migrate to the ciliated portions of the respiratory tract and cleared.

The deposition fraction of unattached radon progeny in the major regions of the human respiratory tract are shown in figure 4.3.

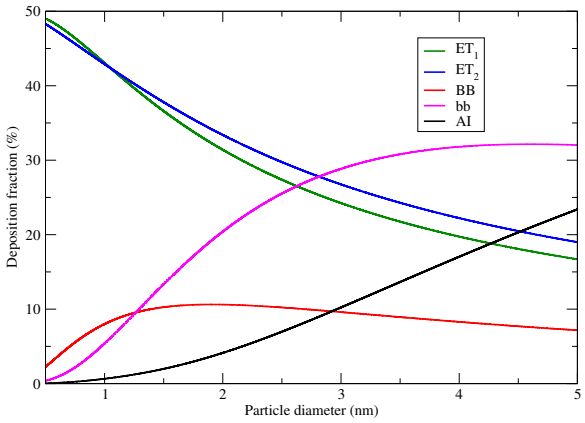

Figure 4.3: Deposition of particles in the major regions of the human respiratory tract.

As can be seen from figure 4.3, deposition for a given particle size differ from region to region, i.e, deposition in upper airways higher for a small aerosol size and it is higher to the lower airway. This is because of the sequential nature of the regions, only those particles that pass through upstream regions have a chance to deposit in downstream regions. In consequence deposition fraction in a downstream region depends not only on the deposition in the region itself but also on the deposition that takes place in upstream regions. During inhalation, the particles that deposit

in the alveolar region are those that have not deposited in the extrathoracic and tracheobronchial regions.

During the pause between inhalation and exhalation, Brownian motion of the particle is negligible.

4.3 Effect of the parameters on deposition fraction

During inhalation, particles are transported with the inspired air through the extrathoracic airways and the bifurcating tracheobronchiolar system to the gas exchange region of the lung. A certain number of these particles deposit in the respiratory system by touching the wet surfaces. There are many parameters for estimation of deposition fraction of unattached radon progeny. Present work uses best the estimation[2] parameters and the correction given by ICRP [3] for estimation of fractional deposition of unattached radon daughters. Values for the parameters are given in table 4.1.

Table 4.1: ICRP66 and the modified parameters.

	Parameters	ICRP 1994	Modified
1	viscosity of air	1.9×10^{-4} poise	1.88×10^{-4} poise
2	Mean free path	0.0712 μm	0.0683 μm
3	Breathing rate	1.2 m^3/h	0.78 m^3/h

1. Extrathoracic region

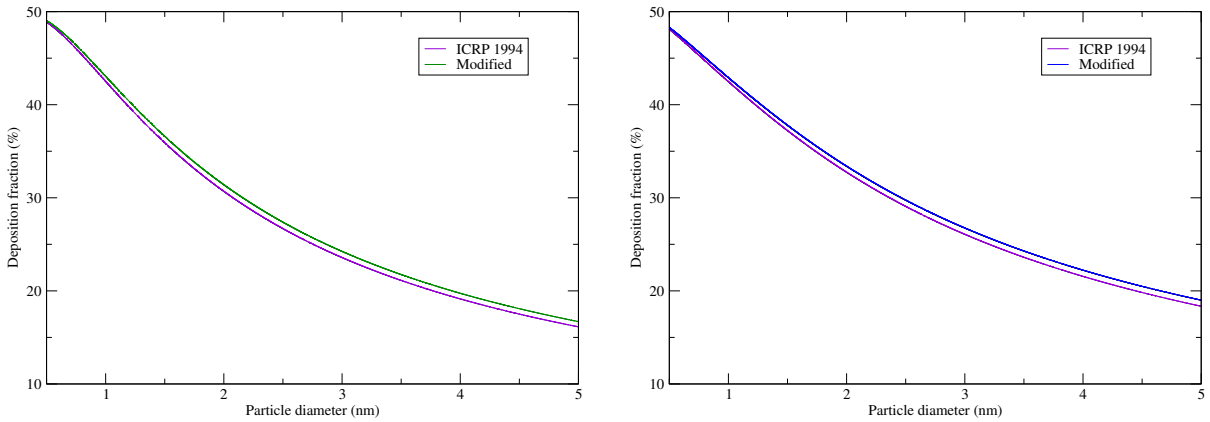

(a) nose **(b)** mouth

Figure 4.4: Deposition fraction for ICRP 1994 and modified parameters in extrathoracic region.

As can be seen from figure 4.4a and 4.4b, the ICRP 1994 predicts underestimate percentage of deposition fraction over unattached aerosol range of 0.5–5 nm.

[2] [40]
[3] http://www.icrp.org/docs/P066_errata_in_P_071_JAICRP_25(3-4).pdf

2. Bronchial and bronchiolar region

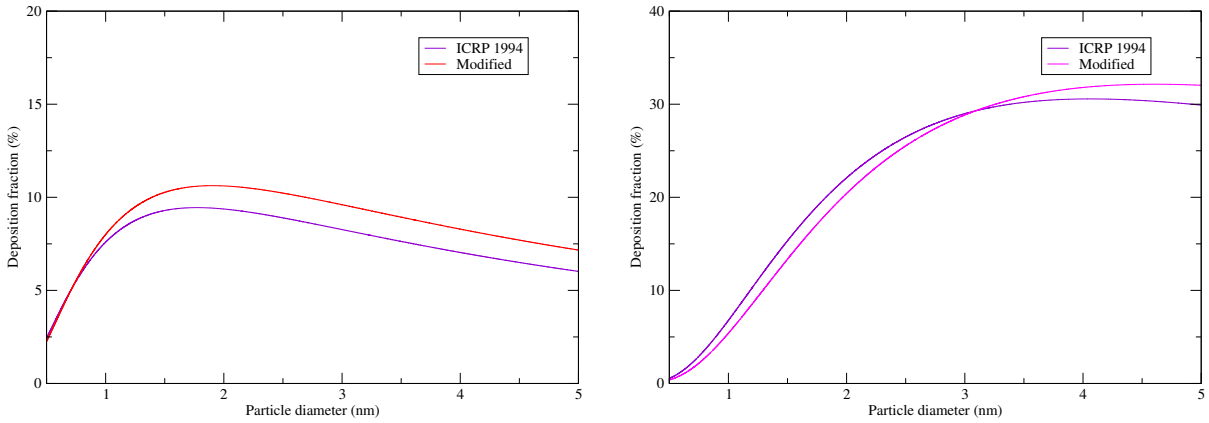

(a) bronchial **(b)** bronchiolar

Figure 4.5: Deposition fraction for ICRP 1994 and modified parameters in tracheobronchial region.

As can be seen from figure 4.5a, the ICRP 1994 predicts underestimate percentage of deposition fraction to the diameter of 0.8–5 nm. For bronchiolar, the ICRP 1994 predicts higher deposition fraction to the diameter range from 0.5–3.1 nm, whereas from 3.2–5 nm it predicts underestimate percentage of deposition fraction 4.5b.

3. Alveolar region and total deposition

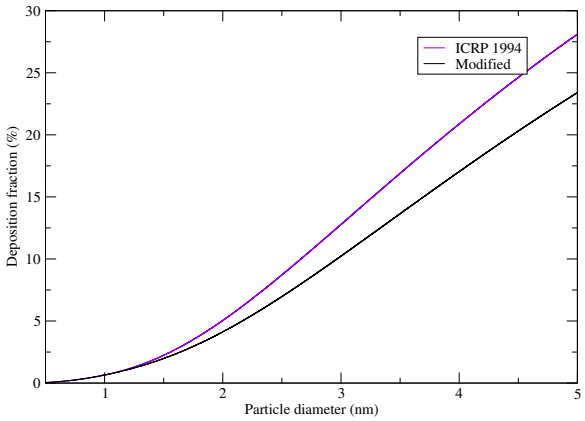

Figure 4.6: Deposition fraction for ICRP 1994 and modified parameters in alveolar region.

As can be seen from figure 4.6, ICRP 1994 predicts exaggerate deposition for unattached diameter in range 1.23–5 nm, but for particle diameter below 1.23 nm they predict the same deposition fraction.

Tables 4.2 summarize the regional deposition fraction of unattached radon decay products for ICRP 1994 and present work.

Table 4.2: Regional deposition for ICRP and present work.

Region	Deposition fraction range (%)					
	Size (nm)	**0.5 -- 1**	**1.5 -- 2**	**2.5 -- 3**	**3.5 -- 4**	**4.5 -- 5**
ET_1	ICRP 1994	48.87—42.51	35.91—30.69	26.69—23.59	21.13—19.14	17.51—16.14
	Modified	49.03 – 43.05	36.60 –31.40	27.38 – 24.24	21.76 – 19.75	18.09 -- 16.70
ET_2	ICRP 1994	48.10—42.48	37.22—32.76	29.09—26.09	23.62—21.57	19.83—18.35
	Modified	48.29 – 42.90	37.80—33.40	29.76—26.77	24.30—22.24	20.50—19.01
BB	ICRP 1994	2.43—7.59	9.28—9.35	8.86—8.22	7.59—6.99	6.46—5.99
	Modified	2.25—8.00	10.25—10.58	10.18—9.55	8.88—8.23	7.64—7.11
bb	ICRP 1994	0.55—6.78	15.33—22.10	26.48—28.99	30.20—30.57	30.40—29.90
	Modified	0.38—5.40	13.35—20.41	25.52—28.84	30.80—31.80	32.14—32.04
AI	ICRP 1994	0.05—0.65	2.24—5.04	8.72—12.78	16.90—20.88	24.63—28.10
	Modified	0.04—0.65	1.98—4.13	6.97—10.22	13.64—17.04	20.31—23.40

From figure 4.4, 4.5, 4.6 and table 4.2, we can observe that modifying of the parameters, underestimate/overestimate the regional deposition fraction. It is important to examine influence of the parameters on deposition fraction.

1. Breathing rate

   From figure 4.7, For extrathoracic region, empirical deposition parameter is $R = D(\dot{V}_n)^{-1/4}$ and deposition efficiency is given by $\eta_{th} = 1 - e^{-aR^p}$. The higher breathing rate, the lower the empirical deposition parameter and deposition efficiency. The deposition fraction for 1.2 m^3/h is lower than the 0.78 m^3/h breathing rate as in figure 4.7a and 4.7b.

   From figure 4.7c, 4.7d and 4.7e For thoracic region, the transit time for 0.78 m^3/h breathing rate is 0.128 sec, 0.123 sec and 1.065 sec, whereas 1.2 m^3/h breathing rate is 88.35 $m$sec, 84.74 $m$sec and 1.723 sec in bronchial, bronchiolar and alveolar region respectively. The higher the transit time, the higher the deposition fraction.

   During inhalation, the air that penetrates to the deepest part of the lungs is the residual air remaining in the dead space when the previous breath ends. The fronts of freshly inspired aerosol spend longer times in the lungs

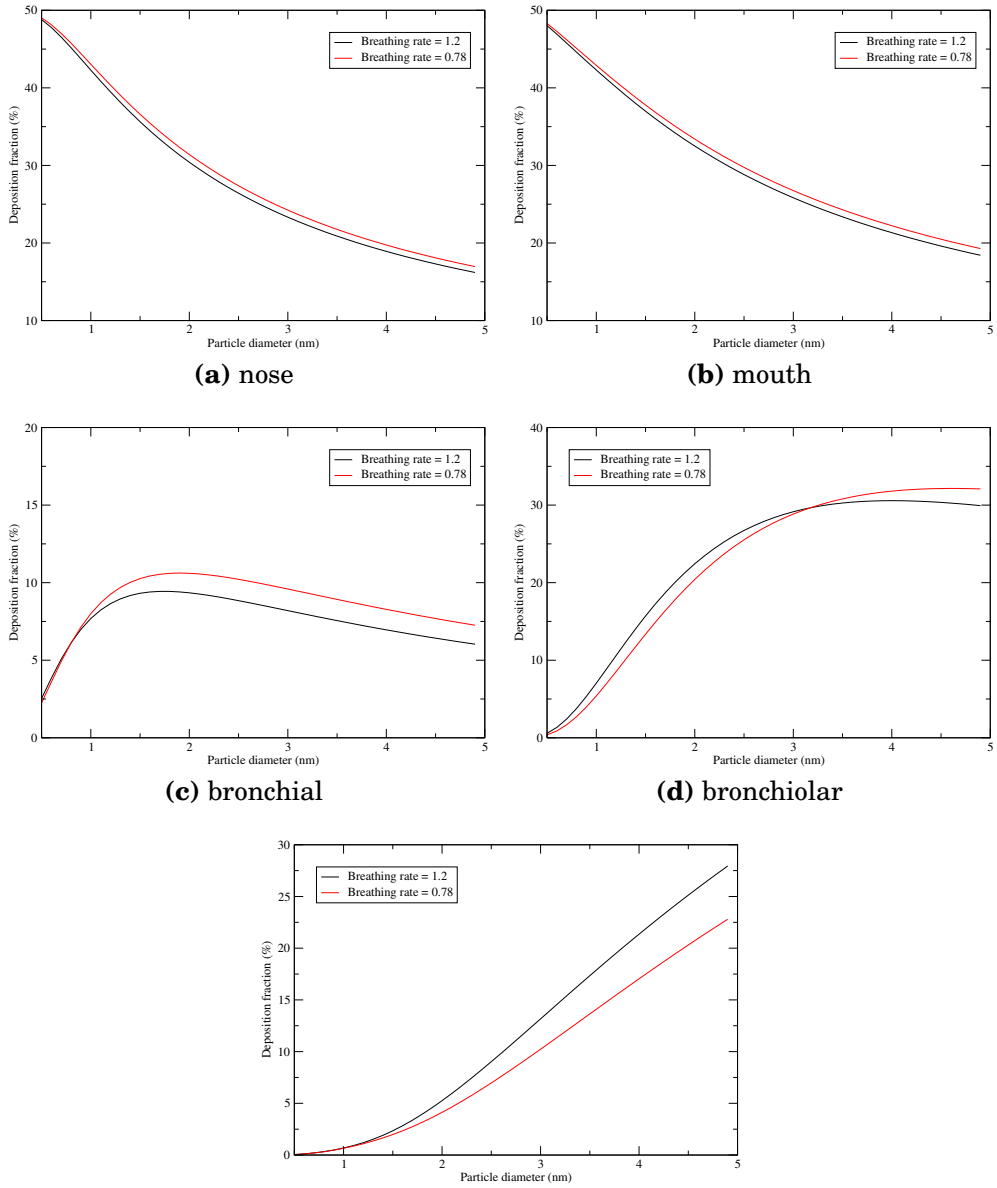

(a) nose **(b)** mouth

(c) bronchial **(d)** bronchiolar

(e) alveolar

Figure 4.7: Effects of the ICRP 1994 and modified breathing rate on deposition.

and reach smaller airways such as alveolar ducts. Some freshly inspired particles deposit on airway walls as they move along the respiratory tract, but none of them have a chance to deposit in alveoli because Brownian motion is not sufficiently fast to move them into expanding alveoli. The particles that deposit in the alveoli are those already in the residual air that is pushed into alveoli by freshly inspired air. The increase in tidal volume brings a larger proportion of tidal air into smaller airways, thereby leading to higher deposition of unattached aerosol by Brownian motion in alveolar.

2. Viscosity

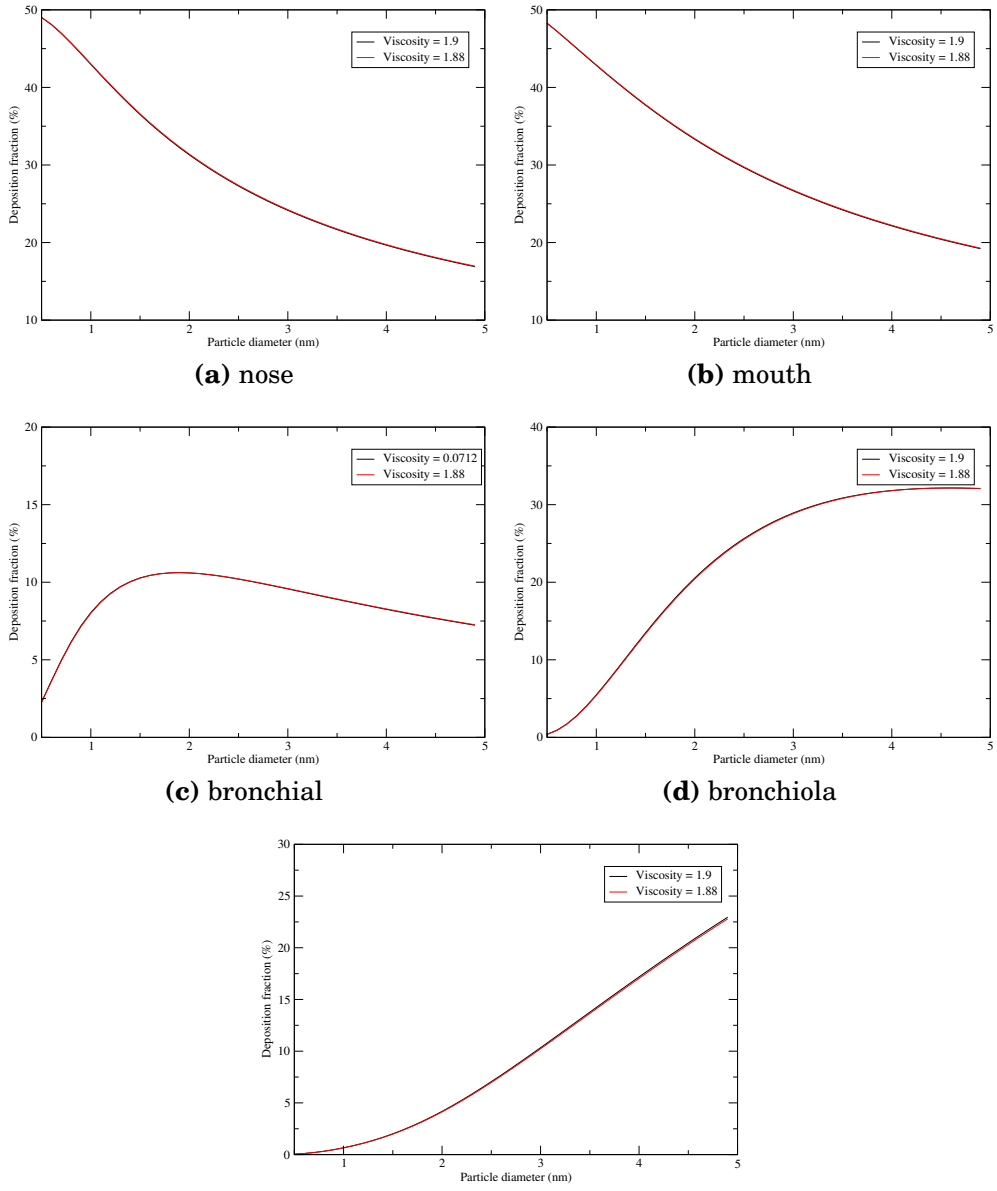

(a) nose **(b)** mouth

(c) bronchial **(d)** bronchiola

(e) alveolar

Figure 4.8: Effects of the ICRP 1994 and modified viscosity of air on deposition.

Since dynamic viscosity of air has an inverse relation with diffusion coefficient, however, the deposition not affected by modified dynamic viscosity of air as in figure 4.8.

3. Mean free path

As can be seen from figure 4.9, the modified mean free path of air molecules has less significant effect on deposition fraction.

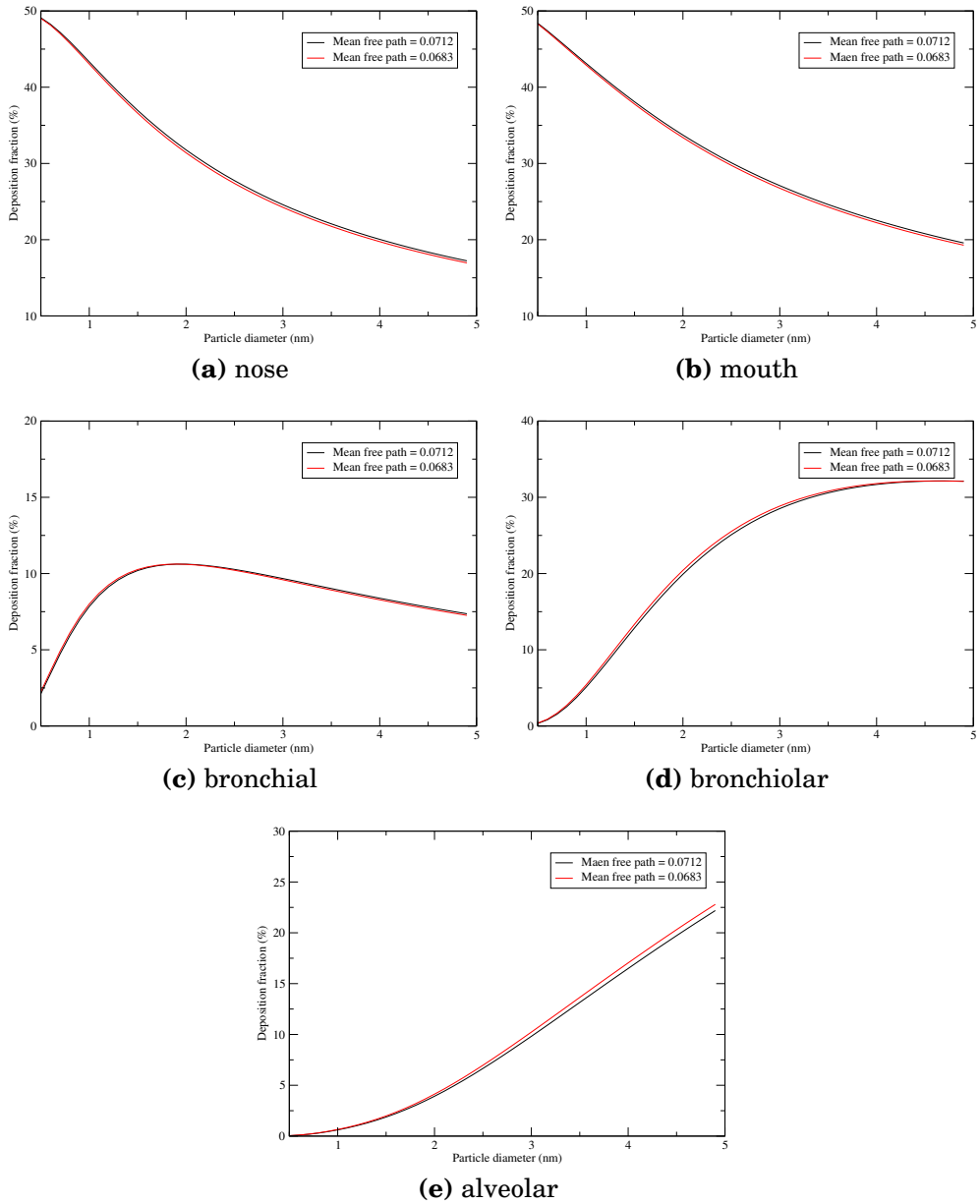

Figure 4.9: Effects of the ICRP 1994 and modified mean free path of air molecule on deposition.

CHAPTER 5

Conclusions and Recommendations

5.1 Conclusions

Over the past half century, a considerable amount of work has been done to the understanding of particle deposition in the human respiratory tract. Although individuals have a considerable degree of variability in the morphology of their respiratory system and breathing pattern. From the values of these parameters, breathing rate has a significant effect on regional deposition fraction unattached radon in human respiratory tract. Deposition by Brownian diffusion increases with increasing residence time and decreasing airway dimension. The effect of increased flow rate was to decrease the extrathoracic deposition fraction and to increase the alveolar deposition fraction for any given particle size.

The extrathoracic and tracheobronchial regions provide a relatively effective defence to prevent alveolar deposition of unattached radon decay products.

5.2 Recommendations

For anyone who interested to work in this area, we recommend that, the present work estimates the deposition fraction as a function of particle size. However, literatures show that deposition rates are significantly higher in an airway bifurcation than in a straight tube and cancer cells are developed on these bifurcation. Therefore it is better to estimate the deposition fraction as a function of airway generation by using the best estimation of aerosol size 0.9 nm. Because this aerosol size has a diffusion coefficient of 0.07 cm^2/sec which is in best agreement with diffusion coefficient for gases based on the kinetic theory.

APPENDIX A
Fortran code for deposition of radon progeny

A.1 Fortran code for deposition of radon progeny

```
1
2 !        AUTHOR. D. NIKEZIC, UNIVERSITY OF KRAGUJEVAC, SERBIA AND MONTENEGRO
3 !        MODIFIED BY ABDU SEID, ADDIS ABABA UNIVERSITY, ETHIOPIA
4 !                   Created on April 21, 2018, 7:56 PM
5
6 !   THIS PROGRAM CALCULATES THE REGIONAL AND TOTAL DEPOSITION FRACTION OF UNATTACHED
7 !   RADON PROGENY IN HUMAN RESPIRATORY TRACT BY USING ICRP66 ALGEBRAIC FORMULAS.
8
9 integer, parameter :: temp = 310
10 integer, parameter :: FRC = 3300
11 integer, parameter :: breathing_freq = 15
12 integer, parameter :: concentration = 3700
13 integer, parameter :: vd_ET = 50, vd_BB = 49, vd_bbb = 47
14 double precision :: dp = 5d-10
15 double precision, parameter :: v_p_h = 0.78d0
16 double precision, parameter :: viscosity = 1.88d-5, lambda = 0.0683d-6, boltz_con = 1.38d-23
17 double precision :: d_th, D, Diffusion_coefficient
18 double precision :: dep_ET1, dep_ET2, dep_BB, dep_bbb, dep_AI
19 double precision :: ave_ET1, ave_ET2, ave_BB, ave_bbb, ave_AI, total_dep
20 double precision :: v_p_s, t_B, t_bb, t_A
21 double precision :: pi
22
23 pi = 4*atan(1d0)
24
25 open(98, file='dep_ET1.dat')
26 open(99, file='dep_ET2.dat')
27 open(100, file='dep_BB.dat')
28 open(101, file='dep_bbb.dat')
29 open(102, file='dep_AI.dat')
30 open(103, file='dep_tot.dat')
31
32 v_p_m = v_p_h*1000/60
33 v_p_s = 2*v_p_m*1000/60
34 vtidal = v_p_m*1000/breathing_freq
35 a_inhaled = concentration*vtidal
36
37 print*, 'volumetric flow rate =', v_p_s
38 print*, 'tidal volume  =', vtidal
39
40 !calculate the transit time of air in regions
```

```
41 t_B = (vd_BB/v_p_s)*(1 + 0.5*vtidal/FRC)
42 t_bb = (vd_bbb/v_p_s)*(1 + 0.5*vtidal/FRC)
43 t_A = (vtidal - vd_ET - (vd_BB + vd_bbb)*(1 + vtidal/FRC))/v_p_s
44
45 print*, 'transit time of air in bronchial = ', t_B
46 print*, 'transit time of air in bronchiolar = ', t_bb
47 print*, 'transit time of air in alveolar = ', t_A
48
49 !calculate the volumetric fractions
50 vd_BB_prim = vd_BB*(1 + vtidal/FRC)
51 vd_bbb_prim = vd_bbb*(1 + vtidal/FRC)
52
53 v_ET1 = 1
54 v_ET2 = 1
55 vol_BB = 1 - vd_ET/vtidal
56 vol_bbb = 1 - (vd_ET + vd_BB_prim)/vtidal
57 vol_AI = 1 - (vd_ET + vd_BB_prim + vd_bbb_prim)/vtidal
58
59 do while (dp .le. 5.1d-9)
60
61 !Cunningham slip factor
62  cunningham = 1 + lambda/dp*(2.514 + 0.800*exp(-0.55*dp/lambda))
63
64 !particle diffusion coefficient (in m^2/sec)
65  D = cunningham*boltz_con*temp/(3*pi*viscosity*dp)
66
67 !particle diffusion coefficient (in cm^2/sec)
68  Diffusion_coefficient = D * 1d4
69
70 !correction of thermodynamic particle diameter
71  d_th = dp*(1 + 3*exp(-2.2*1d3*dp))
72
73 !calculate deposition efficiency
74 call ET1 (Diffusion_coefficient, v_p_s, dep_ET1)
75 call ET2 (Diffusion_coefficient, v_p_s, dep_ET2)
76 call BB (Diffusion_coefficient, d_th, t_B, dep_BB)
77 call bbb (Diffusion_coefficient, t_bb, dep_bbb)
78 call AI (Diffusion_coefficient, t_A, dep_AI)
79
80 !regional deposition efficieny
```

```
F_dep_ET1 = dep_ET1
F_dep_ET2 = dep_ET2
F_dep_BB = dep_BB
F_dep_bbb = dep_bbb
F_dep_AI = dep_AI

!calculate deposition during inspiration
activity_ET1 = F_dep_ET1 * a_inhaled
activity_after_ET1 = a_inhaled - activity_ET1

activity_ET2 = F_dep_ET2 * activity_after_ET1
activity_after_ET2 = activity_after_ET1 - activity_ET2

activity_to_BB = vol_BB * activity_after_ET2
activity_BB = F_dep_BB * activity_to_BB
activity_after_BB = activity_after_ET2 - activity_BB

activity_to_bbb = vol_bbb * activity_after_BB
activity_bbb = F_dep_bbb * activity_to_bbb
activity_after_bbb = activity_after_BB - activity_bbb

activity_to_AI = vol_AI * activity_after_bbb
activity_AI = F_dep_AI * activity_to_AI
activity_after_AI = activity_after_bbb - activity_AI

!calculate deposition during expiration
activity_to_bbb_e = vol_bbb * activity_after_AI
activity_bbb_e = F_dep_bbb * activity_to_bbb_e
activity_after_bbb_e = activity_after_AI - activity_bbb_e

activity_to_BB_e = vol_BB * activity_after_bb_e
activity_BB_e = F_dep_BB * activity_to_BB_e
activity_after_BB_e = activity_after_bbb_e - activity_BB_e

activity_ET2_e = F_dep_ET2 * activity_after_BB_e
activity_after_ET2_e = activity_after_BB_e - activity_ET2_e

activity_ET1_e = F_dep_ET1 * activity_after_ET2_e

dep_ET1_tot = (activity_ET1 + activity_ET1_e) * 100/a_inhaled
```

```
121 dep_ET2_tot = (activity_ET2 + activity_ET2_e) * 100/a_inhaled
122 dep_BB_tot = (activity_BB + activity_BB_e) * 100/a_inhaled
123 dep_bbb_tot = (activity_bbb + activity_bbb_e) * 100/a_inhaled
124 dep_AI_tot = activity_AI * 100/a_inhaled
125
126 dep_tot = dep_ET1_tot + dep_ET2_tot + dep_BB_tot + dep_bbb_tot + dep_AI_tot
127
128 write(98,*) dp*1d9, dep_ET1_tot
129 write(99,*) dp*1d9, dep_ET2_tot
130 write(100,*) dp*1d9, dep_BB_tot
131 write(101,*) dp*1d9, dep_bbb_tot
132 write(102,*) dp*1d9, dep_AI_tot
133 write(103,*) dp*1d9, dep_tot
134
135 dp = dp + 5d-10
136
137 end do
138
139 end
140
141 !************************************************
142 subroutine ET1 (D, vps, b)
143 !deposition efficiency in ET1 region
144 double precision, parameter :: a = 18d0, p = 0.5d0
145 double precision ::  r, vps, D, b
146
147 r = D*vps**(-0.25)
148 b = 0.5*(1 - exp(-a*r**p))
149
150 return
151 end subroutine ET1
152 !************************************************
153 subroutine ET2 (D, vps, b)
154 !deposition efficiency in ET2 region
155 double precision, parameter :: a = 15.1d0, p = 0.538d0
156 double precision ::  r, vps, D, b
157
158 r = D*vps**(-0.25)
159 b = (1 - exp(-a*r**p))
160
```

```
161 return
162 end subroutine ET2
163 !************************************************
164 subroutine BB (D, dth, tB, b)
165 !deposition efficiency in BB region
166 double precision, parameter :: p = 0.6391d0
167 double precision :: psi, a, r, D, tB, b, dth
168
169 !empirical correction factor
170 psi = 1 + 100*exp(-(log10(100 + 10/(dth**0.9)))**2)
171
172 a = 22.02*psi
173 r = D*tB
174 b = 1 - exp(-a*r**p)
175
176 return
177 end subroutine BB
178 !************************************************
179 subroutine bbb (D, tbb, b)
180 !deposition efficiency in bb region
181 double precision, parameter :: a = 167d0 - 76.8d0, p = 0.5676d0
182 double precision ::  r, tbb, D, b
183
184 r = D*tbb
185 b = 1 - exp(-a*r**p)
186
187 return
188 end subroutine bbb
189 !************************************************
190 subroutine AI (D, tA, b)
191 !deposition efficiency in AI region
192 double precision, parameter :: a = 170d0 + 103d0, p = 0.6101d0
193 double precision ::  r, tA, D, b
194
195 r = D*tA
196 b = 1 - exp(-a*r**p)
197
198 return
199 end subroutine AI
200 !************************************************
```

Bibliography

[1] J Ford. Radiation, people and the environment. 2004.

[2] Thomas K. Gaisser. *Cosmic Rays and Particle Physics*. CAMBRIDGE UNIVERSITY PRESS, 1990.

[3] Ionizing radiation exposure of the population of the united states. Recommendations of the NATIONAL COUNCIL ON RADIATION PROTECTION AND MEASUREMENTS 160, National Council on Radiation Protection and Measurements 7910 Woodmont Avenue, Suite 400 / Bethesda, MD 20814-3095, March 2009.

[4] Joakim Pagels, Rolf Falk, Anders Gudmundsson, and Mats Bohgard. Deposition of particle-attached radon progeny in the respiratory tract - an experimental study of children and adults in home environments. LUTMDN/TMAT-3015-SE Publication 60, Lund University, 1999.

[5] James E. Martin. *Physics for Radiation Protection*. Wiley, 3 edition, 2012.

[6] A.C. Chamberlain and E.D Dyson. The dose to trachea and bronchi from the decay products of radon and thoron. *British J. Radiol*, 29:317, 1956.

[7] Mark Baskaran. *Radon: A tracer for geological, geophysical and geochemical studies*. Springer, 2016.

[8] Marvin Wilkening. *Radon in the Environment*, volume 40. Elsevier, 1990.

[9] Kenneth S Krane and David Halliday. *Introductory nuclear physics*, volume 465. Wiley New York, 1988.

[10] Tatjana Jevremovic. *Nuclear Principles in Engineering*. Springer US, 2 edition, 2009.

[11] William R Hendee and E Russell Ritenour. *Medical imaging physics*. Year Book Medical Pub, 1992.

[12] J. Kenneth Shultis and Richard E. Faw. *Fundamentals of Nuclear Science and Engineering*. Marcel Dekker, 2002.

[13] Lars Von der Wense. *On the Direct Detection of 229m Th*. Springer Theses. Springer International Publishing, 1 edition, 2018.

[14] James P Me Laughlin. Natural radiation hazards: Radon in the home and the workplace. 1996.

[15] J Porstendörfer. Properties and behaviour of radon and thoron and their decay products in the air. *Journal of Aerosol Science*, 25(2):219–263, 1994.

[16] Arthur C Chamberlain. *Radioactive aerosols*, volume 3. Cambridge University Press, 2004.

[17] Mark L Maiello; Mark D Hoover. *Radioactive air sampling methods*. CRC Press, 2011.

[18] National Research Council et al. *Health effects of exposure to low levels of ionizing radiation: BEIR V*, volume 5. National Academies, 1990.

[19] Yung-Sung Cheng, TR Chen, HC Yeh, J Bigu, R Holub, K Tu, EO Knutsond, and R Falk. Intercomparison of activity size distribution of thoron progeny and a mixture of radon and thoron progeny. *Journal of environmental radioactivity*, 51(1):59–78, 2000.

[20] KN Yu, BMF Lau, and D Nikezic. Assessment of environmental radon hazard using human respiratory tract models. *Journal of hazardous materials*, 132(1):98–110, 2006.

[21] A Mohammed. Activity size distributions of short lived radon progeny in indoor air. *Radiation protection dosimetry*, 86(2):139–145, 1999.

[22] National Research Council et al. *Comparative dosimetry of radon in mines and homes*. National Academies Press, 1991.

[23] Renate Winkler-Heil, Werner Hofmann, James Marsh, and Alan Birchall. Comparison of radon lung dosimetry models for the estimation of dose uncertainties. *Radiation protection dosimetry*, 127(1-4):27–30, 2007.

[24] James E Turner. Chemical and biological effects of radiation. *Atoms, Radiation, and Radiation Protection, Third Edition*, pages 399–447, 1996.

[25] Syed Naeem Ahmed. *Physics and engineering of radiation detection*. Academic Press, 2007.

[26] Haydee Domenech. *Radiation Safety*. Springer, 2016.

[27] Daniel J Strom. Health impacts from acute radiation exposure. Technical report, Pacific Northwest National Laboratory (PNNL), Richland, WA (US), 2003.

[28] K Eckerman, J Harrison, HG Menzel, CH Clement, et al. Icrp publication 119: compendium of dose coefficients based on icrp publication 60. *Annals of the ICRP*, 42(4):e1–e130, 2013.

[29] Dale L Bailey, JL Huum, Andrew Todd-Pokropek, A Van Aswegen, et al. *Nuclear medicine physics: a handbook for teachers and students*. Vienna: International Atomic Energy Agency (IAEA), 2014.

[30] Karl Heinrich Lieser. *Nuclear and radiochemistry: fundamentals and applications*. John Wiley & Sons, 2008.

[31] Pramod Kulkarni, Paul A Baron, and Klaus Willeke. *Aerosol measurement: principles, techniques, and applications*. John Wiley & Sons, 2011.

[32] Constantin Papastefanou. *Radioactive Aerosols*. 2008.

[33] Daniela Gurau, Doru Stanga, and Mitica Dragusin. Review of the principal mechanism of radon in the environment. *Rom*, pages 9–10, 2014.

[34] Michael G Stabin. *Radiation protection and dosimetry: an introduction to health physics*. Springer Science & Business Media, 2007.

[35] C Richard Cothern and James E Smith Jr. *Environmental radon*, volume 35. Springer Science & Business Media, 2013.

[36] M Roy, MH Becquemin, J 0F Bertholon, and A Bouchikhi. Annexe b. respiratory physiology. *Annals of the ICRP*, 24(1-3):167–201, 1994.

[37] Gehr/Heyder. *Particle-Lung Interactions*. Marcel Dekker Ltd, 2000.

[38] ICRP. *Human Respiratory Tract Model for Radiological Protection*. Publication 66. Oxford: Pergamon Press, 1994.

[39] S Tokonami. Determination of the diffusion coefficient of unattached radon progeny with a graded screen array at the eml radon/aerosol chamber. *Radiation protection dosimetry*, 81(4):285–290, 1999.

[40] JW Marsh and A Birchall. Sensitivity analysis of the weighted equivalent lung dose per unit exposure from radon progeny. *Radiation Protection Dosimetry*, 87(3):167–178, 2000.

[41] Barbara Rothen-Rutishauser Fabian Blank Peter Gehr, Christian MÃijhlfeld. *Particle-Lung Interactions, Second Edition*. Lung Biology in Health and Disease. Informa Healthcare, 2 edition, 2009.

[42] Nikezic D and Yu KN. Dosimetric model of human lung and associated computer program. *Indian Journal of Physics*, 83(6):759–775, 2009.

[43] W Li, JQ Xiong, and BS Cohen. The deposition of unattached radon progeny in a tracheobronchial cast as measured with iodine vapor. *Aerosol science and technology*, 28(6):502–510, 1998.

DECLARATION

ADDIS ABABA UNIVERSITY
COLLEGE OF NATURAL AND COMPUTATIONAL SCIENCES
DEPARTMENT OF PHYSICS

MSc Thesis

Deposition analysis of unattached radon decay products in human respiratory tract

Name of Candidate: Abdu Seid Kamil

I the under signed declare that the thesis is my original work and no part of it can be claimed as an intellectual property of anybody else except me and my advisors.

Signature: _____